Review on solar sail technology

Shengping Gong[1] (✉), **Malcolm Macdonald**[2]

1. *School of Aerospace Engineering, Tsinghua University, Beijing, 100084, China*
2. *Department of Mechanical & Aerospace Engineering, University of Strathclyde, Glasgow, Scotland*

ABSTRACT

This paper reviews solar sail trajectory design and dynamics, attitude control, and structural dynamics. Within the area of orbital dynamics, methods relevant to transfer trajectory design and non-Keplerian orbit generation are discussed. Within the area of attitude control, different control strategies, including utilisation of solar radiation pressure and conventional actuators, are discussed. Finally, the methods of modelling structural dynamics during and after deployment are discussed, before considering possible future trends in developing of solar sailing missions.

KEYWORDS

solar sail
orbit
attitude
structure

Review Article

Received: 07 July 2017
Accepted: 21 November 2018

1 Introduction

Since the former Union of Soviet Socialist Republics launched the first artificial satellite in October 1957, humanity has launched both crewed and robotic missions to explore Earth and its Moon, as well as robotic missions to our parent star, the Sun, and every planet in our solar system. Each mission enhances our understanding of the universe, yet traditional chemical and even electric propulsion has limitations due to the requirement of transporting the required propellant. As such more exotic forms of propulsion have long been considered. Space flight is achieved through a momentum exchange process. For a spacecraft propelled by chemical or electric propulsion, the propellant carried by the spacecraft is ejected to gain momentum equivalent to that of the ejected propellant. Consequently, the propellant mass limits the total stored momentum of the spacecraft. Electric propulsion is more efficient than chemical propulsion as the ejected velocity is much higher. However, with electric propulsion it is difficult to produce a large magnitude of thrust due to electric power limitations. An alternative way to change the momentum of a spacecraft is through environment interaction. In this scenario, forces that are often considered perturbations are harnessed for benefit rather than considered an adverse influence. Examples of spacecraft gaining momentum from the environment include gravity assist maneuvers that gain momentum from a large-body such as a planet or moon [1], or aerobraking [2] and aerocapture [3] that exchange momentum with the atmosphere. Solar sails, sometimes called 'sailcraft', and to which this review is focused, gain momentum from solar radiation pressure (SRP), while electric sails [4] and magnetic sails [5] gain momentum from solar wind. Johannes Kepler in 1619 proposed that comet tails are pushed outwards from the Sun due to sunlight. This is one of the first recorded observations that light may exert a force, although the mechanism behind his force was not elucidated. The current theoretical basis for the existence of radiation pressure was found independent of the astronomical theories. The renowned mathematician and physicist James Clerk Maxwell predicted the existence of radiation pressure in 1873 as a consequence of his unified theory of electromagnetic radiation [6]. The first experimental verification of the existence of radiation pressure and the verification of Maxwell's quantitative results came in 1900 [7–9]. Around this period, a number of science fiction authors wrote of spaceships propelled by mirrors,

✉ gongsp@tsinghua.edu.cn

most notably the French authors Faure and Graffigny in 1889. Solar sailing as an engineering principle can be traced back to the Father of Astronautics, Konstantin Tsiolkovsky and Friedrich Zander (Tsander) [10–12]. In 1923, the German rocket pioneer Herman Julius Oberth proposed the concept of reflectors in Earth orbit (Spiegelrakete, or mirror rocket) to illuminate northern regions of Earth and for influencing weather patterns [13]. In 1929, Oberth extended his earlier concept for several applications of orbit transfer, maneuvering and attitude control (Spiegelführung, or Mirror guidance) using mirrors in Earth orbit [14]. Following the initial work by Tsiolkovsky, Tsander and Oberth, the concept of solar sailing appears to have remained largely dormant for over thirty years. In the 1950s the concept was re-invigorated and published once again in popular literature, this time in North America. The first American author to propose solar sailing appears to have been the aeronautical engineer Carl Wiley, writing under the pseudonym Russell Sanders to protect his professional credibility [15].

The concept of solar sailing is the use of solar radiation to propel a spacecraft, potentially providing a continuous acceleration limited only by the lifetime of the sail materials in the space environment, and the sustained and suitable proximity to the Sun. The membrane is packed during launch and deployed in space. The deployed membrane reflects the solar radiation such that it accelerates the spacecraft continuously and indefinitely, subject only to any degradation of the reflective surface, without the need for an on-board propulsion system. The momentum carried by individual photons is extremely small. A solar sail with a perfectly reflective surface will experience approximately 9 N of force per square kilometre of sail located at one astronomical unit (AU) from the Sun, Earth's average solar distance, thus to provide a suitably large momentum transfer the sail must have a large surface area whilst maintaining as low a mass as possible. Adding the impulse due to incident and reflected photons, it is found that the idealised thrust vector is directed normal to the surface of the sail with all incident photons reflected. By controlling the orientation of the sail surface relative to the Sun, orbit energy can be manipulated as desired to slowly but continuously accelerate the spacecraft to accomplish a wide-range of potential missions.

1.1 Organisation of the survey

Much theoretical research and many missions and experiments relevant to solar sailing have been conducted since the concept of solar sailing was proposed. The missions and experiments will be reviewed in Section 2. For the theoretical work, early solar sail research mainly focused on the orbital dynamics. These works can be summarized into two categories. The first is the planetary and interplanetary transfer trajectory design for solar sail. There is a significant quantity of literature describing trajectory optimization of solar sails from the 1950s. The details of these, together with later follow-on work will be reviewed in Section 3. The other category of orbital dynamics research is to use SRP to generate new families of periodic orbits. These orbits are difficult to achieve with a typical spacecraft as they require continuous thrust, greatly increasing the spacecraft's propellant dependency. Such periodic orbits are usually transformed into equilibria by considering the dynamics of the solar sail in a rotating frame of reference. Stationary solutions to the equations of motion in the rotating frame of reference correspond to periodic orbits when viewed from an inertial frame of reference. Many scholars proposed new non-Keplerian periodic orbits and their potential applications. These approaches will be reviewed in Section 4.

Early comparisons of solar sailing with chemical and ion propulsion systems showed that solar sails could match or out perform these systems for a range of mission applications, though the level of assumed technology status is crucial in such comparisons [16]. However, there are many challenges that have to be overcomed before a real solar sail operates in space. An approximate attitude control strategy is one of them, ensuring the direction of force generated by SRP is as designed. The force is completely determined by the sail orientation relative to the sunlight. Therefore, active attitude control is necessary to steer the sail orientation to control the direction of the SRP force. Compared to the work on the orbital dynamics of solar sailing, less has been done on attitude control, the relevant work appears much later. Though the attitude control technology of a typical satellite is mature, considering the large moment of inertia of a solar sail and large SRP disturbance torques, conventional attitude control methods face new challenges. As such, use of SRP to control the attitude of a solar sail is an attractive approach. Literature on solar sail attitude control will be reviewed in Section 5. Another challenge is the structural dynamics of a solar sail. The sail membrane is stowed in a small space before deployment. Therefore, the first step is the successful deployment of the structure. Understanding the deployment dynamics of the structure is essential to the solar sail mission. After deployment, the flexibility of the structure will influence the attitude and orbit. The work about the structural dynamics will be reviewed in Section 6.

2 Technology developments and activities relevant to solar sailing

Actually, SRP exerts a force on all spacecraft in space. The SRP acceleration level is determined by the area-to-mass ratio or areal density of the spacecraft. For a spacecraft with an ideally reflective surface perpendicular to the sunlight, the SRP acceleration can be given by

$$a = \frac{2PA}{m} = \beta \frac{\mu}{R_{\mathrm{S}}^2} = a_{\mathrm{c}} \left(\frac{R_{\mathrm{E}}}{R_{\mathrm{S}}} \right)^2 \tag{1}$$

where P is the SRP; A is the area of the surface; m is the mass; μ is the constant gravitational parameter of the Sun; R_{E} and R_{S} are the distance from the Sun to the Earth and spacecraft, respectively; β is the lightness number, which is the maximum SRP acceleration divided by the Sun's local gravitational acceleration; a_{c} is the characteristic acceleration, which is the maximum SRP acceleration at the 1 AU distance from the Sun. They are related to the areal density or sail loading σ. If the units of the characteristic acceleration and sail loading are mm/s^2 (millimetre/second^2) and g/m^2 (gram/meter^2), respectively, assuming a perfectly reflective membrane, the relationship between them can be given by Ref. [17]:

$$a_c = \frac{9.08}{\sigma} \tag{2}$$

$$\beta = \frac{1.53}{\sigma} \tag{3}$$

The lightness number or characteristic acceleration represents the performance of a solar sail. For a regular small satellite of 4 m^2 and 400 kg, the characteristic acceleration and lightness number are about 9.08×10^{-5} mm/s^2 and 1.53×10^{-5}, respectively. As previously stated, for regular satellites the SRP acceleration is very small and usually regarded as a perturbation. However, despite being relatively small the SRP exerted on solar arrays can be used to aid spacecraft attitude control. In some cases, the SRP may even provide sufficient force to help alleviate a satellite's propellant dependency for some orbital manoeuvres, effectively increasing the lifespan of the satellite. Attitude stabilization of a space vehicle by SRP was first studied in Ref. [18]. The geostationary communications satellite OTS-2 of the European Space Agency used solar flaps for satellite attitude control [19]. India also used reflective devices mounted on communications satellites to offset the SRP torque from their solar arrays [20]. Such solar-pressure attitude control methods are now common place on large geostationary satellites, and have also been implemented on several interplanetary spacecraft [21]. Mariner 10 used a small "kite" (31 cm× 76 cm in area) for attitude manoeuvring. By using the kite solar sail for attitude control, Mariner 10 was able to extend the planned life of the mission science returns [22]. Messenger also used SRP to help control the growth of spacecraft angular momentum, minimizing the perturbations due to thruster momentum off-loads. With intelligent planning and management of the spacecraft attitude and solar array articulations, the force due to SRP was also used directly as a precision trajectory control for the Mercury flybys [23].

A solar sail utilizes SRP for its main propulsion. As such, it needs a larger characteristic acceleration or lightness number than a typical spacecraft would naturally possess. Though many experiments and demonstrations relevant to solar sailing have been conducted, there are no fully functional and high performance solar sail systems at present. NASA-Jet Propulsion Laboratory (JPL) made the first attempt in the 1970s to construct a solar sail to rendezvous with Halley's Comet when it approached Earth in 1986. Though the project was eventually abandoned, working on the project greatly advanced the development of solar sailing. In addition, the work on the preliminary design of the 800 m × 800 m square sail demonstrated that solar sailing was a potentially viable spacecraft-propulsion technique [24]. In 1993, the Russian Space Agency launched Znamya-2, a 20 meter diameter spinning mirror that produced a 5 km wide region of increased luminosity approximate equivalent to a full moon, which traversed Europe from west to east, in many ways this can be thought of as a realization of Oberth's spiegelrakete. Although the purpose of Znamya-2 was not to use SRP for propulsion, the method of its manufacture and deployment shared similarities to that of a solar sail. The reflector encountered large atmospheric drag in a low Earth orbit (LEO), consequently its altitude dropped quickly and it burned up in the atmosphere. The Russian Space Agency planned to launch larger mirrors called Znamya-2.5 and 3, however the program was abandoned after Znamya-2.5 failed [25]. The Japanese Institute of Space and Aeronautical Science used a sounding rocket to successfully test two methods of solar sail spinning deployment in 2004 at altitudes of 122 km and 169 km [26]. The Planetary Society hoped to demonstrate solar sail technology with its Cosmos-1 mission in 2005. Cosmos-1 was launched by a Russian intercontinental ballistic missile from a submarine. If the mission had been successful, it would have been the first fully functional solar sail in space. Unfortunately, the rocket failed to deliver the payload to the intended orbit [27]. In Cologne, in December 1999, the German Aerospace Center, DLR, in association with the European Space Agency (ESA) and INVENT GmbH, deployed a square 20-m solar sail [28, 29]. A controlled and autonomous strategy was developed and demonstrated on ground at system level. The Technology Readiness Level (TRL) measures the maturity of a technology and its readiness for a space application. Engineering models of the hardware were built and the technology is on TRL four, approaching level five. Another recent mission concept proposed by ESA and DLR is the Multiple Near-Earth Objects Rendezvous Mission (MNEORM) using the Gossamer Roadmap Technology [30–33]. The work showed that three NEOs could be rendezvoused within a decade using a moderate performance solar sail.

Solar sailing spacecraft were proposed for NASA's New Millennium Program (NMP) Space Technology 5, 6, and 7 (ST-5, ST-6, and ST-7) competitions [34–36]. NASA commissioned ATK Space Systems and L'Garde to separately develop two different 20-meter solar sails and tested them on the ground in vacuum conditions. Both sail designs were deployed successfully in an one gravity environment and were thought to be scalable to much larger solar sails. The sail technology was not selected for flight. Later, solar sailing was proposed for NASA's NMP ST-9 mission, competing with four other technologies for a flight demonstration [37]. Another solar sail project, Team Encounter, offered the public the opportunity to send messages and memorabilia heading out of the solar system. L'Garde as the sail provider incorporated the 15.4 g/m inflatable and sub-Tg rigidizable boom, the tip vanes for 3-axis attitude control system and 0.9 μm Mylar sail membrane for Team Encounter. The Team Encounter solar sail, scheduled to launch in 2006, would have been $4900\,\mathrm{m}^2$ and have given a characteristic acceleration of $2.26\,\mathrm{mm/s}^2$. In 2004, the primary investor decided to cancel the mission after investing several millions. In 2008, NASA's Ames Research Center launched NanoSail-D to study the deployment of a solar sail-like surface in space [38]. The satellite was lost shortly after launch due to a problem with the rocket. NanoSail-D2 was launched in 2010 [39]. NanoSail-D2 was expected to separate from FASTSAT on December 6, however, successful ejection was not confirmed until January 19, 2011; it is unclear what caused the ejection mechanism to fail. The spacecraft was expected to remain in low-Earth orbit for 70 to 120 days before it burnt up, depending on atmospheric conditions. However, the spacecraft re-entered the atmosphere after 240 days in orbit [40].

L'Garde, working with NASA, intended to develop the Sunjammer mission in 2015. Sunjammer was to demonstrate various technologies, such as deployment, vector control via vanes, and eventually reaching a location near the Earth–Sun L1 Lagrangian point [41]. NASA cancelled the project in October 2014 after investing four years and more than $21 million because its lack of confidence in its contractor's ability to deliver. At present, NASA is planning the mission Near-Earth Asteroid Scout (NEA Scout) to develop a controllable low-cost CubeSat solar sail spacecraft capable of encountering NEAs [42]. The NEA Scout will be one of 13 CubeSats to be carried with the Orion EM-1 mission into a heliocentric orbit in cis-lunar space on the maiden flight of the Space Launch System (SLS) scheduled to launch in 2019. Four 7-meter booms would deploy, unfurling the $83\,\mathrm{m}^2$ aluminized polyimide solar sail to achieve the mission in about 2.5 years [43].

Japan Aerospace Exploration Agency (JAXA) launched the world's first interplanetary solar sail spacecraft called "Interplanetary Kite-craft Accelerated by Radiation Of the Sun" (abbreviated "IKAROS") in May 2010. The IKAROS mission demonstrated four key technologies. They were (i) deployment and control of a large, thin solar sail membrane, (ii) thin-film solar cells integrated into the sail to power the payload, (iii) measurement of acceleration due to SRP on the solar sail, and (iv) attitude control by varying the reflectance of eighty liquid crystal panels embedded in the sail. It is regarded as a milestone in solar sail technology [44]. However, IKAROS's characteristic acceleration was only about $0.006\,\mathrm{mm/s^2}$. After the success of IKAROS, JAXA planned a larger sail to Jupiter and the Trojan asteroids with a stated goal of returning an asteroid sample to Earth in the 2050s. It has to be pointed out that IKAROS and its follow on mission is mainly aiming for electric propulsion, however many of the key technology requirements are similar. After the failure of Cosmos 1, The Planetary Society continued to develop solar sail technology. LightSail-1 completed in-orbit deployment in May 2015. A follow on mission, LightSail-2, is a project to demonstrate controlled solar sailing using a CubeSat with a deployed area of 32 m^2. The launch is scheduled to occur in early 2019 on-board a Falcon Heavy. LightSail-2 will be released into an orbit with an altitude of 720 kilometres, high enough to minimize the effects of atmospheric drag [46]. DeorbitSail was launched on 10 July 2015 [47]. The proposed objective for DeorbitSail was to demonstrate rapid deorbiting using increased aerodynamic drag from the large surface area of the deployed sail in a LEO. However, the team has not been able to deploy the sail. All the missions relevant to solar sailing are summarized in Table 1.

Solar sail technology relies on several key subsystem technologies, including orbit and attitude dynamics and control, deployment strategy, material technology. Many theoretical works have been conducted for orbit and attitude dynamics and control, which will be reviewed in following sections. However, besides IKAROS demonstrating attitude control using reflectivity control devices, other attitude control strategies have never been demonstrated in space. For solar sail deployment, several experiments have been conducted to demonstrate it both on ground and in space. Although several solar sail missions have been launched successfully, including IKAROS, NanoSailD2, Lightsail1, these missions usually aimed at demonstrating subsystems and analogous concepts rather than solar sailing. Consequently, the performance of these missions as a solar sail is poor. A pure solar sail mission usually requires a lower areal density to achieve higher performance.

A typical square sail configuration consists of a reflective sail membrane, a deployable sail support structure, an attitude control subsystem, and bus. Ultra-thin films and low-mass support booms are essential to keep a system-level low areal density. In addition, selection and manufacturing of membrane and boom materials should consider the performance degradation by space environmental factors. At present, the solution is to coat one side of an extremely thin polymeric membrane with a reflective material and the other side with a material that emits heat efficiently. The areal density of commercial film materials is usually larger than $20\,\mathrm{g/m^2}$, which is only acceptable for solar sail technology demonstration missions although even then the applicability and scalability is questioned by some. Polymeric materials should be specifically designed to achieve areal density required for mission performance. Solar sail membranes have been made from Polyimides, such as CP1 for Nanosail-D, ISAS-TPI for IKAROS, and polyesters such as polyethylene terephthalate (Mylar) for the L'Garde solar sail demonstrator. A typical 5 micrometre thick Mylar sail material has an areal density about $7\,\mathrm{g/m^2}$ and the aluminized Kapton films have an areal density as much as $12\,\mathrm{g/m^2}$. The areal density of modern solar-sail membranes varies from 2 to $20\,\mathrm{g/m^2}$ [48]. L'Garde declared that the thinnest membrane material available was $0.9\,\mu\mathrm{m}$ Mylar when they designed the Team Encounter solar sail [49]. The $0.9\,\mu\mathrm{m}$ Mylar was metallized with aluminum on the frontside, black chromium on the backside. The metallized $0.9\,\mu\mathrm{m}$ sail film weighs $1.53\,\mathrm{g/m^2}$; the seams, adhesives, ripstop, grounding straps and sail-boom connection system add less than $0.23\,\mathrm{g/m^2}$. The total areal density will be less than $2\,\mathrm{g/m^2}$. One supporting boom design is the carbon-fiber-reinforced plastic boom. This design leads to a mass per unit length of 15–25 g/m [48]. The density of inflatable-rigidizable booms during Team Encounter design was about 15 g/m [49]. The mass of the bus and payload has to be added to the membrane and boom mass to count for the system-level areal density. Some references reported the system-level areal density for different designs. Two ground demonstration contracts funded by NASA at the beginning of this century developed two prototype solar sail systems to validate design concepts for sail

Table 1 The techniques demonstrated by different missions

Year	Mission or experiment	Space agency	Demonstrated techniques and other information
1973	Mariner 10	NASA	SRP for attitude control (flown, flyby Venus and Mercury)
1976	Halley Rendezvous	NASA	Preliminary mission design (800 m×800 m square)
1978	OTS-2	ESA	SRP for attitude control (flown, GEO stationary satellite)
1993	Znamya	Russian Federal Space Agency	Spinning deployment in space (flown, 20 m spinning disc, 5 mm-thick aluminised PETF film, 22 g/m^2)
1999		DLR, ESA	Ground deployment
2004	MESSENGER	NASA	SRP for fine orbit correction (flown, orbit around Mercury)
2004		JAXA	Spinning deployment in space (flown, 10 m fan and clover type, 7.5 µm ISAS-TPI)
2005	Cosmos 1 (fail)	The Planetary Society	solar sail mission (flown, eight sail blades of 15 m and total area 600 m^2, 5 µm Mylar membrane)
2005		NASA	System-level solar sail ground demonstration (ATK: 20 m square, rigid coilable boom, a sliding mass ACS, 2 µm CP1 membrane; L'Garde: 20 m square, inflatable and rigidizable boom, vane based ACS, 2 µm Mylar membrane)
2006	Team Encounter (cancelled)	L'Garde	Fully functional mission (concept, 4900 m^2 square, 15.4 g/m inflatable-rigidizable beams, 0.9 µm Mylar membrane)
2008, 2010	NanoSail D (fail), NanoSail D2	NASA	Deployment in space (flown, 10 m^2 square, triangular rollable and collapsible booms, 7.5 µm CP1 membrane)
2010	IKAROS	JAXA	Spinning deployment, attitude control, SRP for orbital maneuverer (flown, 14 m square, 7.5 µm ISAS-TPI)
2014	Sunjammer (cancelled)	NASA	Fully functional mission (concept, 1200 m^2 square, 5 µm Kapton membrane)
2015	LightSail1	The Planetary Society	Deployment in space (flown, 32 m^2 square, triangular rollable and collapsible booms, 4.5 µm Mylar membrane)
2015	DeorbitSail (fail)	ESA	Deployment, deorbit using aerodynamic drag (flown, 5 m square, carbon fibre deployable booms, 12.5 µm Kapton membrane)
Present	Lightsail2	The Planetary Society	Deployment in space, attitude control, orbital raising (to be flown, 32 m^2 square, triangular rollable and collapsible booms, 4.5 µm Mylar membrane)
Present	NEA Scout	NASA	Fully functional mission(to be flown, 86 m^2 square, triangular rollable and collapsible booms, 2.5 µm CP1 membrane)

manufacturing, packaging, deployment, attitude control subsystem. The ATK used CP1 sail membrane and rigid coilable boom to achieve an areal density of about 112 g/m^2, including spacecraft bus structure, a sliding mass attitude control system, power, instrument boom [50]. Furthermore, it could be scaled to 11.3 g/m^2 for 100 m design and no payload. L'Garde used Mylar sail membrane and inflatable and cold-temperature rigidizable boom to achieve an areal density of about 30 g/m^2, including vane-based attitude control system. It could be scaled to 14.1 g/m^2 with 50 kg payload and 41.4 kg bus for 100 m design [50]. The Team Encounter mission used a 4900 m^2 square membrane to achieve an areal density of about 3.63 g/m^2, including 3 kg payload, giving a characteristic acceleration of 2.26 mm/s^2 [49]. Using the thinnest membrane (2 g/m^2) and lightest boom (15 g/m) reported in these references, the characteristic acceleration of a solar sail for different sizes and hardware (bus and payload) mass can be evaluated, as shown in Fig. 1.

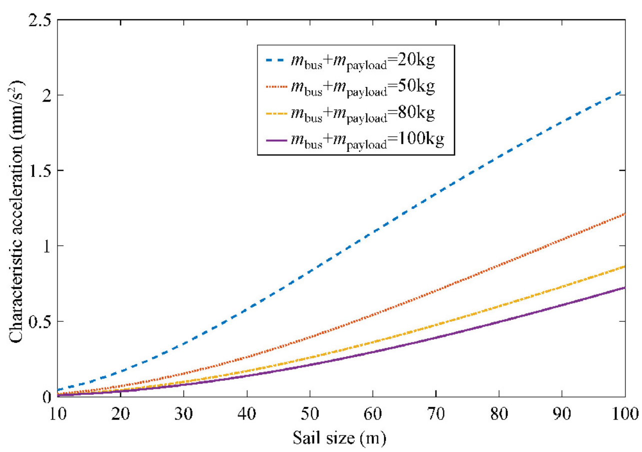

Fig. 1 Characteristic acceleration for different sizes.

It can be seen that it may be possible to design a small sail of 15–30 m size providing a characteristic acceleration of 0.1–0.4 $\mathrm{mm/s^2}$ for some near-term missions. For example, a typical Geosail mission (see below and Fig. 5) with a 10×30 Earth radii orbit in the ecliptic plane requires a characteristic acceleration about 0.135 $\mathrm{mm/s^2}$ that corresponds to the sail loading of about 67 $\mathrm{g/m^2}$. It takes about 2 years for a solar sail of about 0.3 $\mathrm{mm/s^2}$ to rendezvous with Venus. It is also possible for a solar sail of 0.1–0.2 $\mathrm{mm/s^2}$ to visit some near Earth asteroids. However, a large size membrane is required to achieve a high performance solar sail. The size should be larger than 70 m to achieve a characteristic acceleration of about 1 $\mathrm{mm/s^2}$, even for a solar sail with only 20 kg bus and payload mass. It has to be pointed out that the characteristic acceleration cannot be increased inexhaustibly by increasing the size. The maximum value is limited by the areal density of the membrane, where maximum characteristic acceleration is about 4.5 $\mathrm{mm/s^2}$ for a membrane areal density of 2 $\mathrm{g/m^2}$. To achieve even higher performance, some new concepts of solar sail material should be developed. Some such concepts were proposed [51,52]. One of them was using only panels of thin metal films like aluminium, lithium, magnesium and beryllium by removing the polymer. Eric Drexler has developed 30–100 nm thick aluminium sample in the laboratory [52]. However, the material was too delicate to survive from folding, launch, and deployment and should be produced in space. Another new carbon fiber material developed by Energy Science Laboratories might be useful for solar sails. It is so porous that 200 times thicker carbon fiber can provide the same areal density to current conventional solar sail material.

Besides membrane and boom material manufacture, solar sail as a system involves many other complex engineering challenges. The TRL assessment of the L'Garde and ATK component and subsystem fabrication and testing in 2006 documented that both contractors had demonstrated full attainment of the TRL 3 and 4 requirements and partial attainment of the TRL 5 and 6 requirements [53]. NanoSail-D2 by NASA, LightSail-1 by the Planetary Society successfully demonstrated the stowage and deployment of the sail in space, which means the completion of the TRL 6 for relevant subsystems. The NEA Scout mission is being developed, its success will further advance the TRL. JAXA launched IKAROS solar sail mission in 2010, it completed the system demonstration in the space environment, which has taken the TRL to 7. With a new deployment strategy, GOSSAMER-1 by ESA and DLR aims to develop and create a space-qualified scalable technology for the controlled deployment of ultra-lightweight, large film structures in space. It has completed qualification testing including venting, vibration testing, thermal-vacuum testing, ground full deployment, and environmental qualification testing in 2016. The TRL for some components was assessed to be TRL 5 [54].

At present, most flown and planned solar sail demonstration missions are based on mature small satellite bus technologies. The sail subsystems are specially designed to be compatible with the bus. This design is acceptable when the objective is to demonstrate the subsystems in space environment. Based on the experiences from these demonstration missions, the next step may be to design the solar sail spacecraft as a whole, which will advance the TRL to higher levels.

3 Solar sail transfer trajectory design

In interplanetary space, the force generated by SRP is one of the dominant forces exerted on the solar sail. The dynamic equations of solar sail considering the SRP acceleration in the sun-centered two-body problem can be expressed as

$$\begin{cases} \dot{\boldsymbol{r}} = \boldsymbol{v} \\ \dot{\boldsymbol{v}} = -\dfrac{\mu}{r^3}\boldsymbol{r} + \beta\dfrac{\mu}{r^4}(\boldsymbol{r}\cdot\boldsymbol{n})^2\boldsymbol{n} \end{cases} \tag{4}$$

where $\boldsymbol{n}$ is the unit vector along the sail normal. The flight time of the orbit transfer mission is usually used as the performance index because no fuel is consumed for a solar sail. Take the rendezvous problem for example. With the time of departure from the start planet being t_0 and the rendezvous time to the target object being t_f, the initial and final state constraints can be described as

$$\begin{cases} \boldsymbol{r}(t_0) = \boldsymbol{r}_0 \\ \boldsymbol{v}(t_0) = \boldsymbol{v}_0 \end{cases} \tag{5}$$

$$\begin{cases} \boldsymbol{r}(t_f) = \boldsymbol{r}_\mathrm{f} \\ \boldsymbol{v}(t_f) = \boldsymbol{v}_\mathrm{f} \end{cases} \tag{6}$$

where $(\boldsymbol{r}(t_0), \boldsymbol{v}(t_0))$ and $(\boldsymbol{r}(t_\mathrm{f}), \boldsymbol{v}(t_\mathrm{f}))$ are the initial and final states of the solar sail, $(\boldsymbol{r}_0, \boldsymbol{v}_0)$ and $(\boldsymbol{r}_\mathrm{f}, \boldsymbol{v}_\mathrm{f})$ are the states of departure and terminal celestial bodies, respectively.

As the SRP force is constrained anti-sunward, we have another constraint on the control variable $\boldsymbol{n}$ as

$$\boldsymbol{n} \cdot \boldsymbol{r} \geqslant 0 \tag{7}$$

The sail orientation is optimized to obtain the time-optimal transfer trajectory. The performance index J is defined as

$$J = t_{\mathrm{f}} - t_0 = \int_{t_0}^{t_{\mathrm{f}}} \mathrm{d}t \tag{8}$$

The problem is to determine an optimal control $\boldsymbol{n}(t)$ over $t_0 \leqslant t \leqslant t_{\mathrm{f}}$, such that the performance index J is minimized subject to Eq. (4), the boundary conditions Eqs. (5) and (6), and the control constraints Eq. (7).

In the early stages, analytical solutions for transfer trajectories were preferred due to the limitations of numerical techniques and availability of computational systems. The first modern reference for a solar sail appears in *the Journal of Jet Propulsion* in 1958 by Garwin [55]. He studied transfer trajectories between different heliocentric orbits using SRP. A more detailed investigation of heliocentric spiral trajectories was made by Tsu [56], where the planar equations of motion were solved by assuming a solar sail with a fixed orientation. London solved the equations of motion for a solar sail with a fixed orientation with respect to the Sun to find that a solar sail trajectory is a logarithmic spiral [57]. Later, these logarithmic spiral solutions are extended to three-dimensions, series solutions using expansion methods [58]. This logarithmic spiral is not an exact transfer trajectory because the initial and final velocities are discontinuous.

Usually, numerical optimization techniques are required to obtain a minimum-time solution. They are usually categorized as indirect or direct. The indirect method requires the use of the maximum principle to derive the first order necessary condition of the optimal solution. The minimum-time rendezvous problem can be formulated as an optimal-control problem, and the associated optimal-thrust profile can be derived by Pontryagin's maximum principle (PMP) [59]. The Hamiltonian function of the problem is

$$H = 1 + \boldsymbol{\lambda}_{\boldsymbol{r}}(t) \cdot \boldsymbol{v} + \boldsymbol{\lambda}_{\boldsymbol{v}}(t) \cdot \left[-\frac{\mu}{r^3}\boldsymbol{r} + \beta\frac{\mu}{r^4}(\boldsymbol{r} \cdot \boldsymbol{n})^2 \boldsymbol{n}\right] \tag{9}$$

where $\boldsymbol{\lambda}_{\boldsymbol{r}}(t)$ and $\boldsymbol{\lambda}_{\boldsymbol{v}}(t)$ are Lagrange multiplier vectors associated with the position and velocity of the solar sail. The optimal values of the control variables are obtained in the domain of feasible controls by invoking the PMP, that is, by minimizing H at any time. By imposing the necessary condition, one has to optimize $\boldsymbol{n}(t)$ to minimize the Hamiltonian function. Minimizing the Hamilton function means adjusting the sail orientation to minimize the projection of the SRP force along $\boldsymbol{\lambda}_{\boldsymbol{v}}(t)$. In fact, this problem is a locally optimal-type problem [60]. Thus, one knows that the normal vector lies in the plane spanned by the sunlight and $\boldsymbol{\lambda}_{\boldsymbol{v}}(t)$. In the plane, the angle between the sunlight and the sail normal is termed the cone angle and given by Ref. [60]:

$$\alpha = \tan^{-1}\frac{-3 \pm \sqrt{9 + 8\tan^2\tilde{\alpha}}}{4\tan\tilde{\alpha}} \tag{10}$$

where $\tilde{\alpha}$ is the angle between the sunlight direction and $-\boldsymbol{\lambda}_{\boldsymbol{v}}(t)/\lambda_{\boldsymbol{v}}(t)$, as shown in Fig. 2, the optimal-control law can be written in the vector form of

$$\begin{cases} \boldsymbol{n} = \cos\alpha\dfrac{\boldsymbol{r}}{r} + \sin\alpha\boldsymbol{e} \\ -\dfrac{\boldsymbol{\lambda}_{\boldsymbol{v}}}{\lambda_{\boldsymbol{v}}} = \cos\tilde{\alpha}\dfrac{\boldsymbol{r}}{r} + \sin\tilde{\alpha}\boldsymbol{e} \end{cases} \tag{11}$$

where $\boldsymbol{e}$ is a unit vector perpendicular to the sunlight direction.

This particular locally optimal control law maximizes the SRP force along some direction at each instant. The approach itself is particularly useful for planetary escape missions [61]. For earth escape mission, the geocentric energy change is maximized at each instant until the solar sail escapes the Earth.

The time derivatives of the costates are provided by the Euler–Lagrange equations:

$$\begin{cases} \dot{\boldsymbol{\lambda}}_{\boldsymbol{r}} = -\dfrac{\partial H}{\partial \boldsymbol{r}} \\ \dot{\boldsymbol{\lambda}}_{\boldsymbol{v}} = -\dfrac{\partial H}{\partial \boldsymbol{v}} \end{cases} \tag{12}$$

The state differential equation and costate differential

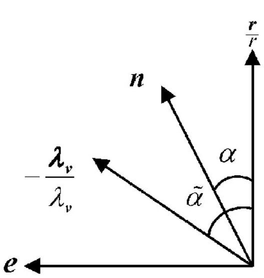

Fig. 2 The optimal-control law description.

equations are coupled via the control parameters. The boundary conditions of the costate are free. The transversality condition are given by

$$H(t_0) = \boldsymbol{\lambda}_{\boldsymbol{r}}(t_0) \cdot \boldsymbol{v}(t_0) - \boldsymbol{\lambda}_{\boldsymbol{v}}(t_0) \cdot \frac{\mu \boldsymbol{r}(t_0)}{r^3(t_0)} \tag{13}$$

$$H(t_{\mathrm{f}}) = \boldsymbol{\lambda}_{\boldsymbol{r}}(t_{\mathrm{f}}) \cdot \boldsymbol{v}(t_{\mathrm{f}}) - \boldsymbol{\lambda}_{\boldsymbol{v}}(t_{\mathrm{f}}) \cdot \frac{\mu \boldsymbol{r}(t_{\mathrm{f}})}{r^3(t_{\mathrm{f}})} \tag{14}$$

Thus, the state and costate equations and the various boundary conditions fully define the optimal rendezvous problem.

It results in a typical two-point boundary value problem (TPBVP), which is equivalent to solving nonlinear algebraic equations. The problem becomes one of finding the departing and final time and initial costates t_0, t_{f}, $\boldsymbol{\lambda}_{\boldsymbol{r}}(t_0)$, $\boldsymbol{\lambda}_{\boldsymbol{v}}(t_0)$ to satisfy the nonlinear algebraic equations (6), (13), and (14). Solving the nonlinear algebraic equations efficiently is nontrivial. The disadvantage of indirect method is that the solution is extremely sensitive to the initial guess. The numerical techniques for trajectory optimization of low-thrust electric propulsion has been widely investigated [62]. The solar sail trajectory optimization is different from that of low-thrust electric propulsion in two ways. Firstly, the fuel-optimal transfer trajectory is usually pursued for low-thrust electric propulsion while the minimum-time transfer trajectory is designed for a solar sail. If an indirect method is employed to obtain optimal solutions, they lead to bang-bang [62] and continuous control laws, respectively. The discontinuity of the bang-bang control of the low-thrust electric propulsion case makes the solution more sensitive to the initial guess of the co-state variables. From this point of view, the trajectory optimization of the low-thrust electric propulsion case is more difficult numerically. Secondly, the direction of the low-thrust electric propulsion is free while the direction of force generated by SRP is constrained anti-sunward. For a perfectly reflective sail it would be directed along the sail plane normal and for a partially reflective sail in-between. In addition, the magnitude of the force varies with the orientation of the sail and the distance of the sail from the Sun. These constraints make the trajectory optimization of solar sails more difficult, and in some cases a desirable solution may not exist [63].

For direct methods, the trajectories are divided into discrete segments and the control laws or states and control laws at discrete points are optimized to obtain a feasible solution satisfying boundary conditions. The scheme will transcribe a continuous dynamic optimization problem to a nonlinear programming (NLP). The advantage of such methods lies in the capability to approximate the optimal trajectory through simple numerical methods, whilst avoiding the difficulty of guessing the initial co-state variables. Although the solution of the NLP does not satisfy the first-order necessary conditions for the optimality, with the optimal controls and optimal trajectory for the NLP, the costates mapping between the continuous optimal control formulation and the NLP formulation can be established using the costates estimation from Karush–Kuhn–Tucker multipliers of the NLP [64]. Here a rendezvous mission with Mars is solved using both indirect and direct method, as shown in Fig. 3. For the direct method, the trajectory is divided into five segments and the pitch angle is assumed constant during each segment and optimized to minimize the flight time while satisfying the boundary conditions. The flight time is about 5 days longer for a total flight time of about 351 days.

Recently, numerical techniques are widely employed to design transfer trajectories for several specific missions, such as Rendezvous missions [33, 65–74], a Solar Polar Imager (SPI) mission [75–82], a pole-sitter mission [83–86] and Geostorm Warning Mission [87–93], an outer solar system mission [94–105], and more.

Many scholars have investigated transfer trajectories for rendezvous missions of terrestrial planets and asteroids/comets. Most studies used the indirect method based upon generalisations of the variational approach to solve the minimum-time transfer trajectory from the Earth to terrestrial planets and asteroids [65–70]. Otten and McInnes used the direct method to show that a small number of fixed attitude steering changes could generate a near minimum-time trajectory [71]. The results again indicated that a small number of fixed attitude steering changes could approximate a near minimum-time trajectory. Mengali combined a classical indirect method with a prescribed discrete number of thrust directions to design transfer trajectories of non-ideal solar sails [72]. Locally optimal control laws were also used to optimize interplanetary transfer trajectories by Macdonald and McInnes [73] and Hokamoto *et al.* [74]. However, an approach based on such control laws is not well suited for the general transfer trajectory problem because it is difficult to

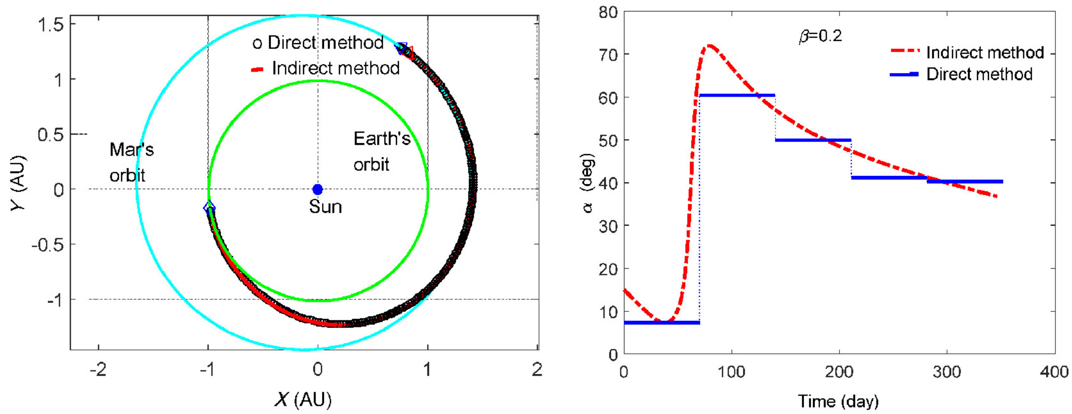

Fig. 3 Comparison between indirect and direct methods for Mars's rendezvous mission.

satisfy the final boundary conditions. At present, the transfer trajectory optimization problem of a single arc has been almost solved. The trajectory optimization problem of the multiple-objective rendezvous is more challenging because of the large number of different possible ordered sequences and difficulty in optimizing a multiple-arc trajectory numerically. Recently, Peloni *et al.* [33] employed the direct method based on a Radau pseudospectral method to solve the transfer trajectory for a multiple-NEA rendezvous mission, using a shape-based approach to select sequences of encounters.

The SPI mission is one of several Sun–Earth connection solar sail roadmap missions envisioned by NASA [75]. The mission requires the spacecraft to evolve in a heliocentric circular orbit that is resonant with Earth and has a high inclination [76]. In 1996, JPL studied a single trajectory phase that had several close approaches to the Sun, which were constrained at a final orbit distance of 0.48 AU. The flight time for the baseline trajectory in the study was nearly three years for a characteristic sail acceleration of $1\,\mathrm{mm/s^2}$ [77]. In order to find trajectories with shorter flight times, Sauer discussed a two phase trajectory scenario that is likely very close to being optimal, where the initial phase of the trajectory delivers the spacecraft to a circular orbit at the desired orbital distance and at an inclination of 15 degrees [78]. The details of the optimization method were not mentioned there, but it mentioned that a single phase would have a very close approach to the Sun for a low-performance solar sail when an indirect method was employed in the optimization process. Dachwald used the Evolutionary Neurocontrol optimization method to obtain a shorter time using temperature as a constraint, where the "Hot" mission scenario generated a much faster transfer than the "Cold" scenario [79]. Mengali combined the locally optimal method and globally optimal approach to produce an approximate solution in the form of interpolating functions. Each phase is studied in a global optimal framework using an indirect approach, and the final trajectory is simply obtained as an orderly sequence of the different phases [80]. Macdonald used orbit averaging techniques to develop analytical approximations of circle-to-circle low-thrust trajectory transfers with plane-change about the Sun [81].

Another application of solar sails is to use SRP to generate non-Keplerian orbits, such as heliocentric and planet-centred displaced orbits and new artificial equilibria in the restricted three-body problem. The heliocentric displaced orbit is proposed to realize the pole sitter mission [82] and the geocentric displaced orbit is proposed for lunar polar observation [83]. McInnes discussed possible transfer schedules between different displaced orbits using impulsive manoeuvres [83]. Hughes designed transfer trajectories from the Earth to a solar displaced orbit using a direct method, where the trajectories are discretized into several segments and the sail orientation is assumed constant during each segment [84]. Since pure solar sail propulsion is difficult to achieve some pole-sitters, Ceriotti *et al.* designed the minimum propellant pole-sitter orbits and the transfer trajectories between north and south pole-sitters using solar electric propulsion and hybrid propulsion [85, 86].

The concept for the Geostorm Warning Mission used a solar sail positioned inside the Earth's L_1 point to improve the warning time for geomagnetic storms [87]. It was suggested that the spacecraft be transported to the classical L_1 libration point where the sail would be deployed [88]. A typical sub-L_1 mission includes a sequence of three phases. The first mission phase consists of the launch of the spacecraft from the Earth to a halo orbit about the Earth–Sun L_1 libration point. During this phase, the propulsive sail membrane of the spacecraft is not yet deployed. The pre-sail-deployment phase terminates in this L_1 halo orbit as risk mitigation: in the event that the sail membrane cannot be deployed, the spacecraft can still work at the L_1 libration point albeit with degraded warning time. The second phase starts with the deployment of the sail membrane and initiation of travel by the spacecraft along a transfer trajectory from the L_1 halo orbit to the vicinity of the targeted sub-L_1 point. The third phase entails station-keeping, keeping the spacecraft in the vicinity of the sub-L_1 point for the remainder of the mission. For the second stage, the indirect method was used to obtain the minimum-time transfer trajectory with 45° cone angle constraint. For a sail whose characteristic acceleration is about $0.3\,\mathrm{mm/s^2}$, it will take about 280 days to fly from the L_1 halo orbit to the target sub-L_1 point region by incorporating a gravity assist manoeuvre [89]. In the restricted three-body problem, the stable and unstable invariant manifold tubes associated with libration point orbits are phase space structures that provide a conduit for spacecraft to and from the smaller primary body and between primary bodies for separate three-body systems [90]. Furthermore, these invariant manifold tubes can be used to produce new techniques for constructing low energy spacecraft trajectories. Similarly, the invariant manifolds exist in the neighbourhood of artificial Lagrange points and the centre manifolds are used to generate periodic orbits around the points [91]. Gong first proposed an invariant manifold associated with solar sailing to design transfer trajectories [92]. The invariant manifolds of solar sails are used to design transfer trajectories from the Earth parking orbits to artificial equilibria and between different equilibria. In another study, invariant manifolds of L_1 and sub-L_1 halo orbits are utilized to achieve transfers from L_1 halo orbit to sub-L_1 region [93].

Solar sails show advantages in missions to the outer solar system and even beyond although SRP decreases with the square of solar distance. NASA's Interstellar Program began in 1999 after a year of advanced mission and program planning activities [94]. NASA evaluated propulsion options including electric propulsion, nuclear propulsion, beamed energy sails, and matter-antimatter for interstellar missions, and the results indicated that solar sailing was one of the promising candidates [95]. Most work focused on the conceptual design and technological challenges of these missions [94–97]. The NASA-JPL solar sail interstellar mission studies have focused largely on the use of high-performance spin-stabilized disc solar sails, exhibiting a characteristic acceleration of approximately $3\,\mathrm{mm/s^2}$ [98]. A number of novel fast heliopause trajectories have also been presented, using a strategy of orbital angular momentum reversal [126]. The propulsive capabilities of a solar sail will be greatly reduced by proceeding into the outer regions of the solar system. Consequently, continuous outward spiralling to reach the outer solar system is not an efficient method. A solar sail may gain an enormous amount of orbital energy by approaching the Sun before proceeding to the outer solar system. Such a solar assist can greatly reduce the trip time to the outer planets without applying other gravity assists. Therefore, a solar sail usually needs to make one or more close approaches to the Sun to achieve a large cruise speed. Parametric studies of multiple photonic assists have also been conducted by NASA-JPL for missions to Pluto and the Kuiper belt, which could be extended to approximate the Heliopause scenario [95]. Dachwald studied minimum-time trajectories to the outer planets and into near interstellar space using Evolutionary Neurocontrol for both ideal and non-ideal sails [99]. The results indicated that the minimum flight time depended both on the characteristic acceleration of the solar sail and the allowed minimum solar distance which was constrained by the temperature limit of the sail film. Lyngvi *et al.* and ESA/ESTEC considered low-performance sails to achieve a slow transit to 200 au with a conventional three-axis-stabilized square sail, with composite booms derived from DLR, German Aerospace Center activities [100–102]. In particular, a 21.2 year, $0.75\,\mathrm{mm/s^2}$ ideal sail trajectory has been presented that spirals down to 0.37 AU and then executes a dual photonic assist; however, the closest solar approach is just 0.1 au, placing severe thermal loads on the spacecraft and sail assembly [103]. Macdonald *et al.* considered the sail from Earth departure until it is jettisoned at 5 au, and the solar approach limit is restricted to 0.25 au due to the thermal effects on the sail [104]. Sharma and Scheeres used local control laws to escape the solar system [105]. The angle of the solar sail with respect to the Sun was optimized to maximize the rate of change of the semimajor axis or orbital energy of the solar sail. They also studied escape trajectories with solar assist using this local control law, which was achieved by first spiralling inward towards the Sun at a specified distance from the Sun, then switching to increase orbit energy until escape.

As reviewed above, solar sail transfer trajectory design methods have been widely studied. However, most studies use the ideal solar sail model assuming perfect reflection and only a few use an optical model that considers absorption and diffusion. In addition, optical properties of thin metalized polymer films may be altered by the erosive effects of the space environment [106,107]. This degradation behaviour and its potential effects on trajectory have rarely been considered during trajectory design. The work of Dachwald and Sznajder may be a first step in this direction. Furthermore, if the degradation effect is not slowly but instantaneous under certain conditions, the impact is different compared to the studies. In practical applications, a large pitch angle will reduce the efficiency of force generated by SRP greatly and there would not be enough SRP torque for attitude control. Therefore, the pitch angle should not be too large [108]. In addition, attitude angle variation should not be too fast to guarantee that the attitude control system is able to maintain the required trajectory. The best way is to use orbit–attitude coupling dynamics to plan attitude control actuation directly, instead of using attitude angles to design the transfer trajectory, which will be onerous in terms of computation time due to the multiscale problem in the coupling equation.

4 Solar sail non-Keplerian orbits

Keplerian orbits only exist by neglecting all perturbations. Using this definition, all spacecraft experience non-Keplerian orbits. This review is focused on a special subset of the non-Keplerian orbits, where only new orbits are reviewed which consider the gravitational force of a centre point mass and force generated by SRP. McKay has reviewed highly non-Keplerian orbits, where some additional accelerating/propelling force over a full orbit is comparable to the sum of the gravitational and centripetal accelerations experienced by the object [109]. The highly non-Keplerian orbits reviewed by Mckay include heliocentric and planet-centric displaced orbits in the two-body case, and equilibria in circular restricted three body cases. Usually, these orbits are obtained by considering the dynamics of the solar sail in a rotating frame of reference. Details about the generation and stability of these orbits can be found in that review, we focus on the non-Keplerian orbits that are not discussed there.

Sun-synchronous orbits are non-Keplerian orbits that typically use the central body's non-spherical shape to precess the orbits ascending node. SPR forces can also be used when the planet is insufficiently non-spherical. To avoid the severe thermal environment when passing near the subsolar point of Mercury's hot surface, Leipold first proposed Mercury Sun-synchronous polar orbits using solar sails [110], as shown in Fig. 4. Considering Mercury's orbital period around the Sun, a Sun-synchronous orbit can be obtained by precessing the longitude of the ascending node. McInnes and Macdonald considered a different type of Sun-synchronous orbits, precessing the argument of perigee, around the Earth in the ecliptic plane and showed that an ellipse will be precessed while leaving the orbit-averaged semi-major axis and eccentricity unchanged [111], as shown in Fig. 5. The elliptical orbit can be forced to precess at a Sun-synchronous rate and thus a science payload may remain longer within the geomagnetic tail, a concept used by the GeoSail mission

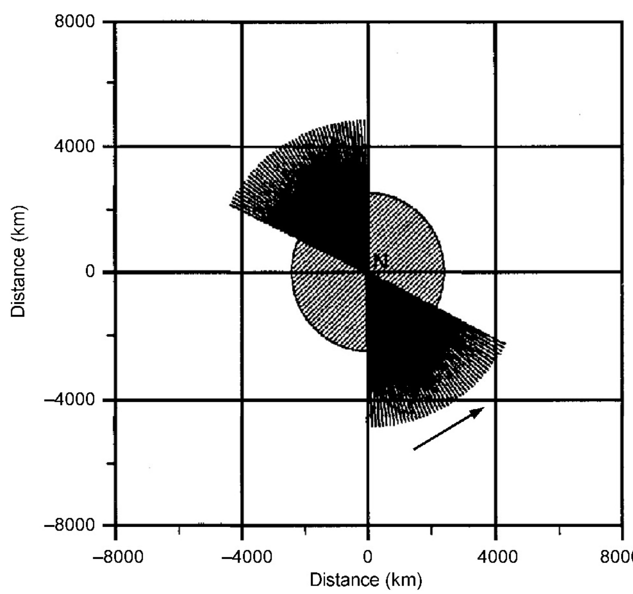

Fig. 4 Progression of the orbital plane about Mercury at perihelion (view from above the north pole for 45 revolutions). Reproduced with permission from Ref. [110], © Elsevier 1994.

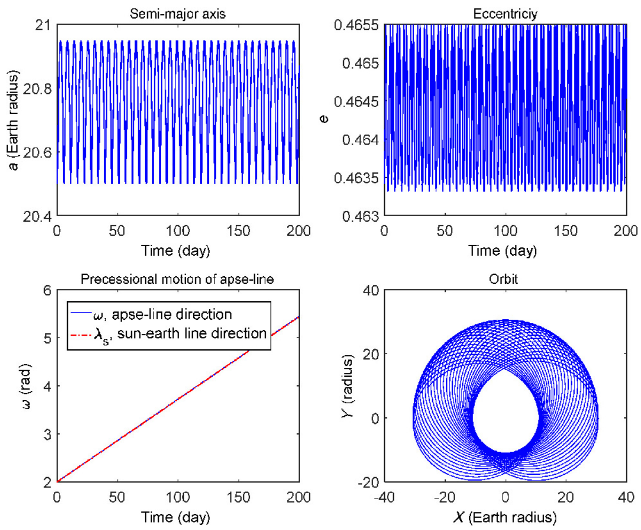

Fig. 5 GeoSail orbit. Reproduced with permission from Ref. [111], © *Journal of Spacecraft and Rockets* 2001.

[112]. To avoid shaded regions, Gong proposed the geocentric Sun-synchronous frozen orbit [113]. These orbits possess the features of both frozen and Sun-synchronous orbits. Attitude can be varied in a small range to prolong the frozen time in an ephemeris model. Tresaco used a double-averaging technique to study frozen orbits around Mercury by considering the nonsphericity of Mercury, the gravitational force of the Sun and SRP [114].

In the review of highly non-Keplerian orbits by Mckay, only circular displaced orbits and equilibria in the circular restricted three body problem (CRTBP) are discussed. However, the orbits of some planets such as Mercury and near Earth asteroids are highly eccentric. A non-uniform rotating frame should be adopted to study the non-Keplerian orbits associated with these bodies, either elliptic heliocentric displaced orbits in two-body problems or equilibria in the elliptic restricted three body problem (ERTBP). Baoyin studied the planar artificial equilibria in a non-uniformly rotating, pulsating coordinate system in the ERTBP and showed that out-of-plane equilibrium surfaces do not exist [115]. Usually, there are two attitude angles, pitch angle and clock angle, that can be most easily adjusted for a solar sail. However, three free variables of solar sails are required to make a solar sail equilibrate at an out-of-plane equilibrium point in the ERTBP because the force balance condition in the out-of-plane direction is time-varying. One way to achieve the out-of-plane equilibrium is to change the sail area. However, it is difficult in engineering practice to change the sail area or characteristic acceleration. In 2010, and as previously discussed, the demonstration mission IKAROS was launched by JAXA. One of the techniques verified was to use reflectivity control devices (RCD) for attitude control. The RCD is mounted on the edge of the sail membrane, and can generate a torque by changing the induced force on each small element's surface by switching between two states [116]. The idea of adjusting the reflectivity states of the RCD for orbit control was proposed by Gong [117–120] and Aliasi [121]. In this case, an elliptic heliocentric displaced orbit is possible in the two-body problem by designing the attitude and reflectivity of the RCD [120], as shown in Fig. 6. Similarly, out-of-plane artificial equilibria in the ERTBP are possible, and even equilibria in the body-fixed rotating frame of an asteroid can be achieved using the RCD [122]. Besides artificial equilibria in the RTBP, new periodic orbits are also feasible. Baoyin described periodic orbits around artificial equilibria on the axis joining the primaries [123]. These periodic orbits are analogous to halo orbits in the CRTBP, as shown in Fig. 7. Biggs and Waters studied the periodic orbits of solar sails around out-of-plane artificial equilibria, as shown in Fig. 8. He first constructs the n^{th}-order approximations to periodic solutions around out-of-

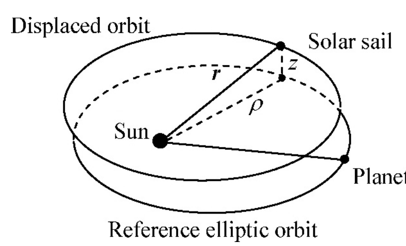

Fig. 6 Elliptic displaced orbit. Reproduced with permission from Ref. [120], © *Journal of Guidance, Control, and Dynamics* 2014.

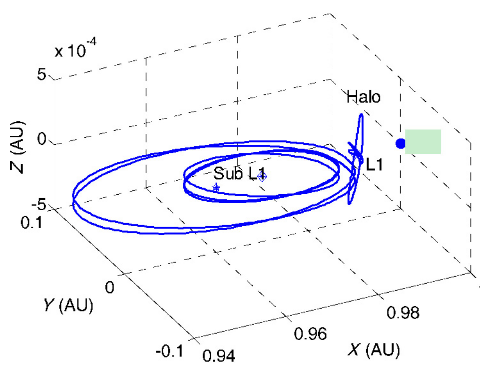

Fig. 7 Periodic orbits near sub-L_1 artificial Lagrange points.

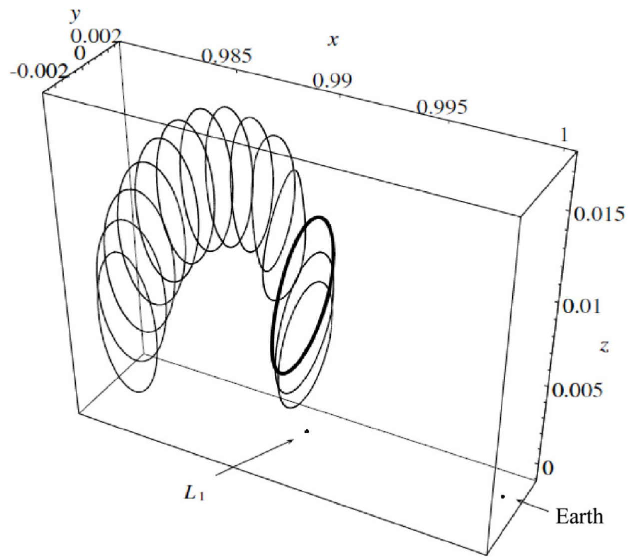

Fig. 8 Periodic orbits around out-of-plane artificial Lagrange points. Reproduced with permission from Ref. [92], © Springer Nature 2011.

plane equilibria using the Lindstedt–Poincare method. Then, a differential corrector algorithm is used to correct the approximations to periodic solutions to the full non-linear system [91]. Biggs *et al.* used numerical continuation methods to construct periodic trajectories in the ERTBP, by using the eccentricity as a perturbation parameter [124]. Gong proposed two families of new out-of-plane periodic orbits in the ERTBP [125]. These periodic orbits staying in the vicinity of out-of-plane fixed points are obtained by seeking special periodic solutions to the equations of motion of a solar sail in the ERTBP.

Another exotic non-Keplerian trajectory for a solar sail is the H-reversal trajectory. H-reversal trajectory means orbital momentum reversal, and the sail's motion changes from prograde to retrograde. Usually, orbital momentum can be reversed by increasing the inclination above 90 degrees, the H-reversal trajectory reverses the momentum in a different way. Orbital momentum is reduced by the SRP until it reaches zero at some point and then reverses, as shown in Fig. 9. During this process, the inclination of the orbit can be kept unchanged. Vulpetti was the first to address the H-reversal trajectory in 1992 in missions to the heliopause and beyond [126]. He considered a high-performance solar sail with a lightness number between 0.5 and 1. He found that a sailcraft, through H-reversal trajectory, was able to achieve a cruise speed considerably higher than its heliocentric speed at the injection from the Earth–Moon system. He investigated both two and three dimensional H-reversal trajectories and applied them for interstellar missions [127, 128]. Due to the H-reversal trajectories requiring very high-performance solar sails, there was little subsequent research on this subject. An H-reversal trajectory was also proposed to escape solar system as an alternative to the solar photonic assist manoeuvre [129]. Recently, some new features and applications of the H-reversal trajectory have been proposed. The minimum sail lightness number to achieve an H-reversal trajectory with fixed attitude has also been determined [130]. The double H-reversal, referred to as the "H2-reversal trajectory" (H2RT), periodic orbit was discovered accidentally within fixed cone angle and optimal control theory [131], as shown in Fig. 10. Several new applications of H-reversal trajectories have also been proposed [132]. The first application was to use the H2RT for space observation. The second application was to use the H-reversal trajectory for heliocentric transfers. A third application was to use the H-reversal trajectory to collide with highly potential dangerous asteroids near the Earth [133]. The trajectory in H-reversal mode was able to produce high crash energy in a head-on impact.

Many new orbits for solar sails have been discovered since the concept of the solar sail was proposed and this work will continue. The significance of discovering new orbits can be viewed from two different perspectives. From the perspective of scientific research, seeking new orbits is always a pursuit of those dedicated to celestial mechanics. Discovery of new orbits is always

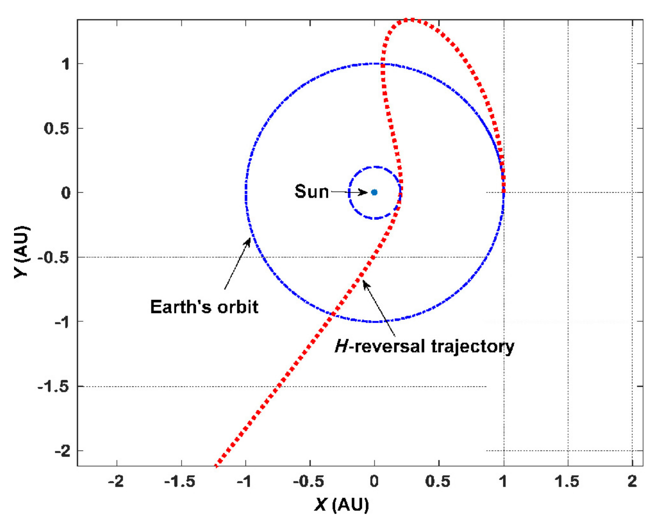

Fig. 9 H-reversal trajectory. Reproduced with permission from Ref. [130], © *Science China Technological Sciences* 2011.

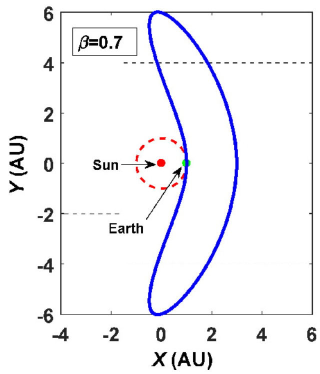

Fig. 10 Double H-reversal trajectory. Reproduced with permission from Ref. [132], © *Research in Astronomy and Astrophysics* 2011.

encouraging. Examples of such work include Suvakov and Dmitrasinovic discovering 13 new solutions to the three-body problem [134], and Hamilton discovering fresh solutions to the four-body problem [135]. From the perspective of engineering practice, the objective of seeking new orbits is to support mission concepts. Therefore, seeking new orbits is demanded by a mission's scientific objectives. Several new orbits of solar sailing belong to this case. Examples include sun-synchronous orbits for the GeoSail mission, artificial equilibria for the GeoStorm mission, and heliocentric displaced orbits for the Polar Observer mission.

5 Attitude control

Active attitude control is required to steer a sail orientation relative to the sunlight as a means to control the direction of the force generated by SRP. There are two categories of active attitude control techniques: using SRP, or conventional actuators, such as reaction wheels to generate control torques.

The key feature of a solar sail is its lack of propellant. It follows that it would be desirable to control the whole sail through propellant-free means. If active attitude control relies on conventional techniques it will diminish the value of propellant-free propulsion, as discussed by Wie [136, 137]. A centre of mass (cm) and centre of pressure (cp) offset will always exists on a solar sail due to manufacturing and deployment tolerances and errors. The SRP disturbance torques induced by this cm/cp offset can therefore be used by the attitude control system to maintain the desired attitude. Wie determined that a 40 m $\times$ 40 m, 160 kg sailcraft with a nominal solar-pressure force of 0.01 N and a cm/cp offset of ± 0.1 m had a solar-pressure disturbance torque of ± 0.001 Nm, which is about 100 times larger than that of typical geosynchronous communications satellites [136]. In addition, a solar sail usually has a large moment of inertia due to its mass distribution. Large active control torques are therefore required for attitude manoeuvres due to large moments of inertia. A conventional three-axis attitude control system will require large reaction wheels, and a prohibitively large amount of propellant, to counter such a major disturbance torque acting on the solar sail. Long duration missions are enabled due to the propellant-free nature of solar sail, but carrying fuel and actuators of large mass diminishes this.

In light of the technology readiness level of solar sails at present, mission risks, and demonstration mission objectives, it could be considered to choose a conventional ACS that includes reliable, and flight-proven actuators for demonstration missions. Beginning missions with propellant-free techniques such as gimbaled tip vanes and a movable mass may be considered too risky, since they are unproven techniques for attitude control. Several conventional attitude control techniques are proposed for some demonstration missions. Steyn proposed using a nano Y-momentum wheel to stabilize a 5 m $\times$ 5 m solar sail in the DeOrbitSail project [138]. Jordaan and Steyn designed a control mechanism for his proposed tri-spin solar sail in low Earth orbit by using 3-dimensional magnetic control and two reaction wheels [139]. Polites described an attitude control scheme for the solar sail baselined for the ST-9 mission using small reaction wheels and magnetic torquers [140], which were previously thought impractical for solar sail attitude control because of the large disturbance torques due to the cm/cp offset. However, he argued that the disturbance torques could be kept small by choosing the right orbit and constraining the attitude of the solar sail, making these actuators feasible to control the attitude of a solar sail for some demonstrations.

In practice, as propellant or energy is consumed, conventional methods are suggested as a secondary/backup system to be used for recovery from off-nominal conditions such as when the Sun angle exceeds the primary ACS limits. Wie studied attitude control using reaction wheels for an Earth orbiting solar sail [141], but found that a too large momentum wheel was required to counter SRP and orbital-disturbance torques. Another approach is to use tip-mounted thrusters for attitude control. The advantage of using tip-mounted thrusters is that a long moment arm can be achieved. The disadvantage is that fuel lines and cables routed through the booms will greatly increase deployment complexity. Micro Pulsed Plasma Thruster (PPT) is potentially a better option because of its smaller size and power needs. Wie studied PPT performance requirements for solar sails and designed a pulse-modulated PPT control as an additional control mechanism [141].

For all these reasons, the primary ACS of a solar sail would most-likely rely on propellant-free methods. At present, many techniques have been proposed to generate control torques using SRP. Attitude control of solar sail is similar to solar-pressure attitude control of ordinary spacecraft. The methods can be classified into three categories including adjustment of cm, adjustment of cp, and passive stability design. For methods of cm and cp adjustment, accessories or mechanisms are used to change the relative cm/cp to generate the desired control torques. For passive stability methods, the configuration of the solar sail, including its mass distribution and the shape of its membrane, are designed to keep a desired attitude relative to the sunlight. As such, the design seeks to ensure that restoring torques are generated to return the deviated attitude to the desired one.

5.1 Attitude control by adjusting centre of pressure

A lot of actuators for adjusting cp have been proposed. Based on the ST5 Geo-storm solar sail of NASA, Wie [136] investigated the attitude dynamics of a simplified one-axis solar sail with control vanes, as shown in Fig. 11. The control vanes were installed at the tips of booms and thus the moment arms were large and the required vane area can be small. The research indicated that vane-steering logic law had a singularity problem and thus may require additional control actuators. On the other hand, by considering a zero pitch angle case, orientation of the solar sail can be passively stable by the correct arrangement of control vanes. Another approach actively shifts and tilts vanes that comprise the sail in order to generate torques for three-axis attitude control as proposed for ST-6. Lawrence *et al.* [142] investigated the control performance of four large vanes on the tip of the booms of solar sail. The research showed that full 3-axis attitude control can be achieved independently by vanes with an assumption of area variation. Mettler *et al.* [143] applied a simplified allocation strategy to obtain the attitude control law for solar sails with articulated vanes. In general, the problems of the control vanes method include the complexity of the whole configuration and the risk of deployment. Instead of adjusting the cp with small flaps, Wie [137] proposed a 3-axis attitude control method adjusting cp by shifting and tilting sail panels. The sail panels can be radially translated for pitch/yaw control and twisted by the rotation of spreader bars at the end of the booms for roll control. Although this attitude control method proved feasible, the requirements for the precision of the translating sail panel and the twisting of the spreader bars are high. Another method to change the cp is to use four bus mounted movable solar panels. The advantage of bus mounted solar panels over boom mounted ones is the small deployment risk, but shadows on the sail film produced by large solar panels and the small moment arm will decrease the sail performance. Generally speaking, the mass of the attitude control actuators will increase as the size of solar sail gets larger. Fu *et al.* [144, 145] proposed an idea for attitude control of a square 3-axis stabilised solar sail without the use of actuators whose mass increase with sail size. It was assumed that the attachment point connecting the membrane and boom can be shifted and thus the sail membrane can take on a curved contour under the influence of force generated by SRP. The cm/cp offset induced by the curved membrane can be used for attitude control. The mathematical relationship between the shift of attachment point, the cm/cp offset and the attitude control torque were derived and the control torque was estimated to demonstrate the feasibility of this method. But this methodology was developed under an ideal static sail film shape without considering the actual dynamics of the sail membrane and a more precise model was needed to validate the qualitative conclusion in the paper. Another thought for changing the cp is to modulate the reflectivity rate of the membrane without adding mechanical systems to change the shape or the area of the sail membrane, which was successfully demonstrated by JAXA's IKAROS [145]. The reflective control system (RCS) consists of Liquid Crystal Devices (LCD) which control the reflectivity to generate SRP torques for attitude control. RCS devices almost avoid the oscillation induced by the attitude manoeuvre and

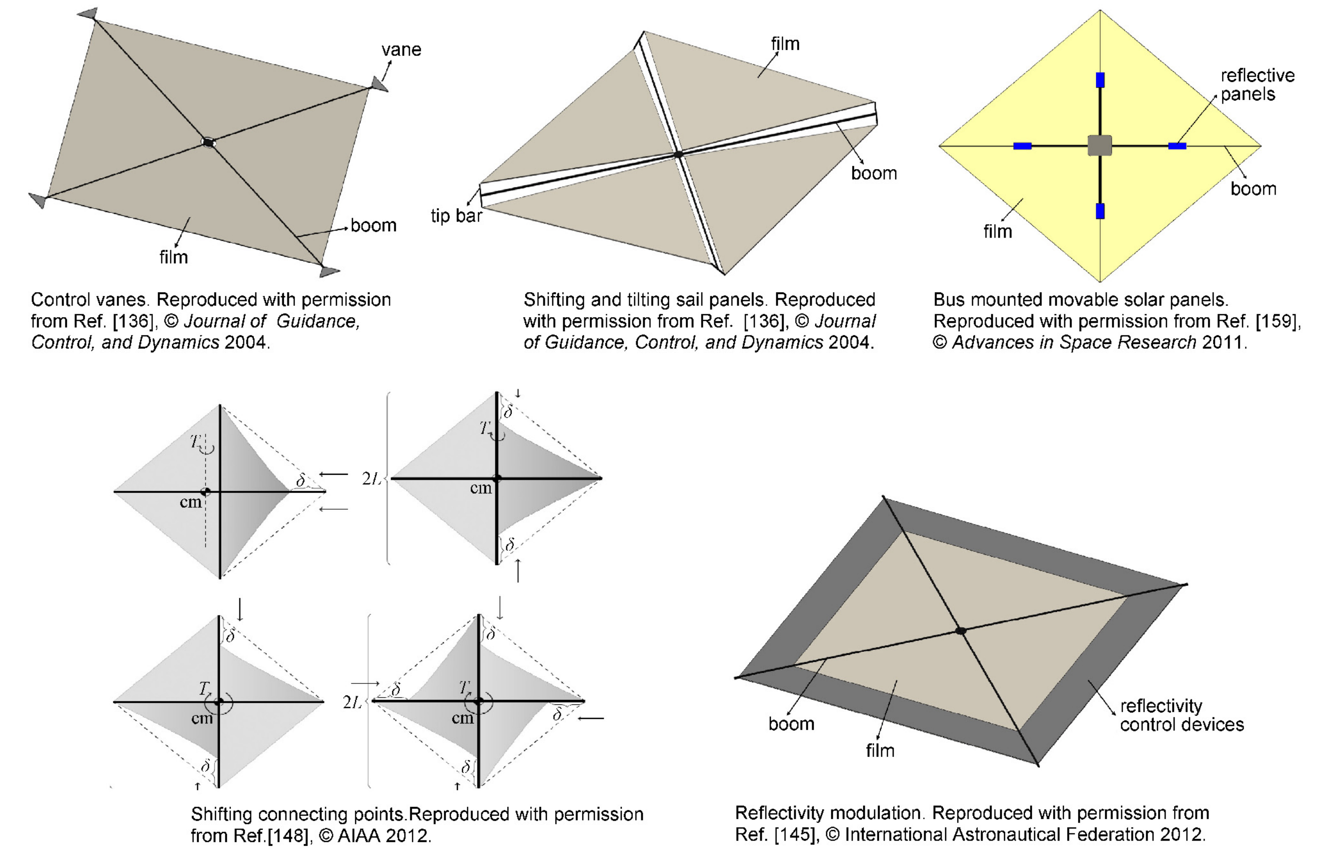

Fig. 11 Different methods for adjusting cp.

can provide enough control torque for a large solar sail. But these devices increase the weight of sail system and thus lighter RCS material is desirable. Funase *et al.* [147] derived a precise torque model for RCS attitude control considering arbitrary sail shape and deformation and the validity of the model was demonstrated by on flight data from IKAROS. After the success of IKAROS, other researchers also investigated RCS control based on the pioneering work by the JAXA research team. Guerrant *et al.* [148] investigated reflectivity control of a small-scale spin heliogyro demonstrator solar sail and made a sensitivity study to assess the control permanence of LCD devices. Mu *et al.* investigated a reflectivity-controlled solar sail formation for a magnetosphere mission and indicated that the reflectivity modulation parameter can be used directly as a control variable for trajectory-track problems in addition to the original attitude control purpose. Borggräfe *et al.* [149] studied the optimal attitude control of solar sails using variable reflectivity distribution achieved by electro-chromic elements across the sail film.

Consequently, the use of control vanes, sail panel translation/rotation, or reflectivity modulation is usually able to achieve three-axis attitude control of sailcraft. There are also some special cases where the control law may be singular as discussed by Wie [137]. In these cases, additional actuators should be provided to avoid the singularity.

5.2 Attitude control by adjusting center of mass

One way of achieving cm/cp offset is through changing the position of the cm of the solar sail system. The center-of-mass adjustment techniques do not operate on sail film and are decoupled from the sail oscillation, but the disadvantage is that they will add extra mass to the system. There are two main approaches for cm adjustment: the gimbaled central mast and distribution of masses. The gimbaled control boom method utilizes a 2-axis gimbaled boom with a mass at the tip for pitch/yaw control [150]. The spacecraft bus that contains all of the spacecraft support subsystems can be mounted on one end of a boom. The other end of the boom can be attached to the centre of the sail with a 2-axis gimbal. The boom can then be actively gimbaled in order to move the cm of the spacecraft relative to its cp as proposed for ST-7. For this type of ACS, Diedrich derived an optimal linear quadratic regulator controller [150]. An alternative approach is to mount the spacecraft bus on a two-degree-of-freedom linear translational stage connected to the centre of the solar sail. Actively translating the spacecraft bus relative to the sail moves the spacecraft cm relative to its cp as a way to generate solar radiation torques for pitch-and-yaw control.

The distributed mass method uses small masses that move inside the spacecraft bus or along supported booms. Wie *et al.* presented a 3-axis attitude control method employing two ballast masses running along mast lanyards for pitch/yaw trim control while the roll control was obtained by roll stabilizer bars at the mast tips and this controller was verified by simulations of controlling a 160 m, 450-kg solar sail for the Solar Polar Imager mission [151] and a 40 m, 150 kg solar sail in a 1600 km altitude dawn–dusk Sun-synchronous orbit [152]. Bolle *et al.* [153] achieved 2-axis attitude control of a circular solar sail by means of a small mass moving in the solar sail plane, whereas the roll-axis control was achieved via rotation of ballast with two masses at the extremities. Scholz *et al.* [154] studied two sliding masses moving inside and along mast lanyards for pitch/yaw control. Romagnoli *et al.* [155] presented a high performance 2-axis attitude controller using ballast masses sliding inside the sail's booms. Although many attitude methods have been proposed, it is rare to find literature demonstrating these actuators by experiments.

As the methods of adjusting cm like a gimbaled control boom or control mass transition cannot generate the SRP force in the sail plane, there will be no control torque along the direction perpendicular to the sail plane. Consequently, they can only achieve pitch/yaw control. In order to provide a three-axis attitude control approach, and more control redundancy and more control authority, mixed control methods are preferable. Wie studied a dynamical model equipped with a gimbaled control boom and two or four vanes at the spar tips. He also investigated the attitude control of a simplified pitch-axis model using both a gimbaled boom and a conventional thrust vector. Nasir *et al.* [158] built a trim control mass actuation mechanism to demonstrate a 3-axis attitude control system using a trim control mass actuator to change cm and highly reflective panels to create a windmill torque. Adeli *et al.* [159] achieved 3-axis control by utilizing ballast masses to change the cm for pitch/yaw control and tilting solar panels attached to the bus to change the cp for roll control. For a CubeSat mission in a Sun-synchronous low earth orbit, Steyn *et al.* [160] proposed a robust and low cost 3-axis attitude control system using a combination of a small sail panel shifting in a 2-dimensional plane and magnetic torque.

5.3 Passive stability design

The concept of passive stability exploits SRP torques to produce a stable Sun-pointing attitude [161]. Instead of changing the cm or cp from a control actuation perspective, passive stability seeks geometries that stabilise the solar sail in the presence of SRP. One early solar sail design was a spherical balloon [162]. Kirpichnikov *et al.* studied the stability of a two-folding sail formed by two unequal reflective rectangular plates [163]. The results indicated that this geometry creates a marginally stable Sun-pointing attitude. Kolk *et al.* [164] further developed the configuration into sail geometries consisting of more planar surfaces. Atchison and Peck considered a stable Sun-pointing corner-cube architecture that used three plate-like Sprites [165]. This design makes the three plates' common corner reach an equilibrium angle with respect to the sunlight line.

McInnes [166] showed that the orbit of a solar sail in heliocentric displaced orbit was stable if the solar sail kept a fixed orientation with respect to the sunlight line. It means that both the attitude and orbit can be stabilized passively. Gong *et al.* [167] designed a four-triangle-form solar sail whose orbit and attitude were passively stable. In addition to 3-axis passive attitude control, Gong *et al.* also investigated the passive stability of a spinning solar sail. A flat spinning solar sail was stabilized in a displaced orbit by design of its spinning rate and sail structure [168]. He also proposed a cone configuration solar sail evolving in the heliocentric displaced orbit and pointed out that the attitude can be passively stable by designing its shape parameters [169]. Kreissl *et al.* [170] explored the passive attitude stability of a square sail supported by booms in deep space. It was found that the attitude of such a sail can be stabilized passively if

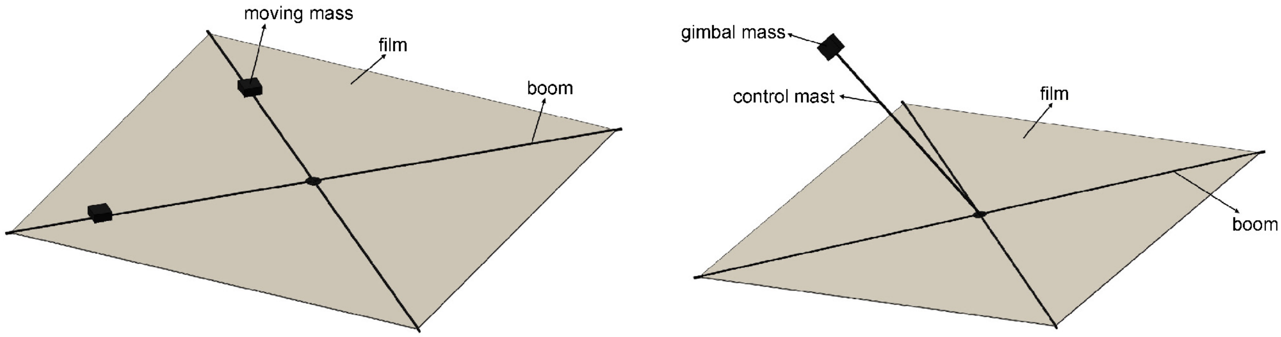

Gimbaled control boom. Reproduced with permission from Ref. [156], © Rocket Propulsion: Present and Future 2003.

Moving mass. Reproduced with permission from Ref. [157], © *Progress in Aerospace Sciences* 2016.

Fig. 12 Different methods for adjusting cm.

the square sail is designed to be slightly conical-shaped. This requirement for passive stability is easily achieved through engineering. However, the author obtained the conical shape numerically, which did not provide general criteria for designing the shape. Hu *et al.* [171] used the linear stability theory to derive general passive stability criteria for 3-axis stabilization axisymmetric curved solar sails, such as conical and parabolic shapes. Using these criteria, a spinning solar sail able to increasing the orbital inclination passively was designed [172].

A large volume of work on numerical simulations has been done to show the feasibility of different propellant-free ACSs. Most of these simulation works regard solar sails as rigid bodies and do not consider their flexibility. Solar sails are usually very flexible and the deformation may be large. The fuel-free attitude control actuators are usually attached to solar sail and the influences of the deformation of the boom and membrane on different actuators are rarely discussed. In addition, attitude control actuators may excite vibration in the solar sail though the natural frequency of a large solar sail is very low. Since it is difficult to test an attitude control system on the ground, it is more important to establish high fidelity models to verify these ACSs. The structural dynamics of solar sails should be incorporated into these models. The structural dynamics can be modelled precisely with ground experiments. Then, use of the attitude-structure coupling dynamics to verify different ACSs is more convincing.

6 Structural dynamics

The prediction of the dynamic response of the solar sail during the deployment as well as in the flight is one of the most important technology for the system design. Solar sail is first packed into a small size to fit into a launch vehicle and then deployed to a functional sail after released from the launch vehicle. The successful deployment is the first step of a solar sail mission. After deployment, the sail is usually very thin and flexible. Since the SRP thrust generated by sail is directly affected by the shape of the reflective surface, the changes in the sail thrust associated with the structural dynamics are of great importance. Firstly, the structure should be rigid enough to keep the sail from collapse or large deformation due to external loads because large structure deformation will diminish sail performance. Small deformations even wrinkle in membranes may make the SRP force and torque different from those of the ideal planar sail. In addition, wrinkles can significantly affect a membrane structure's static and dynamic responses. Another problem associated with structural dynamics is the vibratory motion of the sail, which may lead to instability of the structure, attitude and orbit.

The dynamic responses of the solar sail greatly depend on structural design, the type of attitude stabilization, and the folding and packing pattern. Several different sail design concepts have been proposed [173]. These different design concepts include a square solar sail whose membranes are typically stretched between four equal-length support booms, a heliogyro solar sail consisting of several blades connected to the bus, a disc solar sail that employs several radial spars to support a circular disc of reflective surface, a solar sail like IKAROS that has no boom or spars. For square solar sail, the support boom design is important to the dynamic responses because the load created by the SRP is supported entirely by the booms. The booms should be rigid enough to support the load and also light in mass as larger mass is detrimental to the sail's propulsion performance. The method of the membrane suspended to the boom is another factor that influences the dynamic responses. For the spinning solar sail like heliogyro, disc solar sail and IKAROS, the centrifugal force from spinning is used for deployment, stiffening and stabilization. One of the main advantages with spinning solar sail is that the significant forces are in the plane of rotation, and the tension in the membrane can be adjusted by the spin rate.

In this survey, we will not discuss the structural designs and folding and packing patterns. We focus on methods to model and analyze the structural dynamics. We will not discuss methods associated with heliogyro solar sail since Wilkie *et al.* have given a detailed review on the structural dynamics [174]. Compared to other large space structures, a solar sail that uses centripetal forces or long booms to deploy and tension its membrane is structurally unique. The booms are very long and flexible and the membrane is very thin and extremely large. These long booms and large thin membrane induce several challenges of modeling the solar sail. The long flexible boom leads to large deflection at the end of the boom. In addition, a thin membrane has zero out-of-plane stiffness unless there is in-plane tension. The membrane will wrinkle because it is impossible to achieve absolutely uniform in-plane tension. In recent years, a lot of works have been conducted to study the structural dynamics of solar sail. The methods to study structural dynamics may be classified into two categories: analytical methods, numerical methods. Several simplified analytical models have been proposed for the spinning solar sail. However, it is difficult to use analytical methods only to solve the structural dynamics of a square solar sail in a closed-form way because the design parameters are usually very complex. The advantage of an analytical method is that it allows wide application in the design of control schemes and qualitative analysis. However, numerical methods are necessary either to evaluate the validity of analytical methods or to predict more accurate dynamic responses because ground testing of full-scale large solar sails is impractical due to gravity.

6.1 Analytical method

In early studies of the solar sail spin deployment technique, Ferdor [175] made a two-dimensional analysis of a Yo-Yo de-spinner. Collins [176] extended the analytical model to a three-dimensional case. Based on Ferdor's model, Gardsback *et al.* [177–179] studied the analytical description of the one-step deployment of a rotating web or membrane folded into arms coiled around a central hub using a two-dimensional model. This simple model was used to describe the deployment dynamics qualitatively and obtain the control requirement for centrifugal deployment. It should be noted that several assumptions were made in deriving this analytical model, such as the lack of out-of-plane motion, nutation dynamics and energy dissipation caused by deformation were also not considered. As such, many improvements can be made to this simple analytical model, such as including elasticity. Based on Collins's model, Haraguchi *et al.* [180] carried out a series of three-dimensional transient analyses of a one-step spin deployment using a simple analytical model consisting of a rigid body and four cables with tip masses. In the model, the mass of membrane band was ignored and he adopted the assumption of a symmetric distribution membrane band in the deployment process. Wei *et al.* [181] studied a two-step deployment method using a three-dimensional analytical model considering the nutation dynamics and the mass of the membrane band. On the basis of this model, proper structural parameters were presented to maintain the successful deployment with small nutation angle and avoid re-wrapping around the hub.

The dynamic responses of the solar sail are still important after the sail is fully deployed. In the design of IKAROS, many analytical flexible models of spinning sail membranes were proposed. Nakano *et al.* [182] proposed an analytical one-order vibration model of a spinning thin plate without any external forces. This model was often used for the controller design and the qualitative analysis of the sail's motion [183, 184]. Okuizumi [185–187] investigated the static deflections and vibration modes of a rotating circular membrane subjected to transverse distributed loads utilizing an analytical method called the von Karman theory [188]. The author showed that this method could be used to estimate the approximate equilibrium states and modal frequencies. Mori *et al.* [189] utilized the first mode model of out-of-plane deformation to analyse the oscillation mode of a spinning solar sail and showed this model was simple and valid for the design of the attitude controller. Sugita *et al.* [190] introduced a mathematical dynamics model including

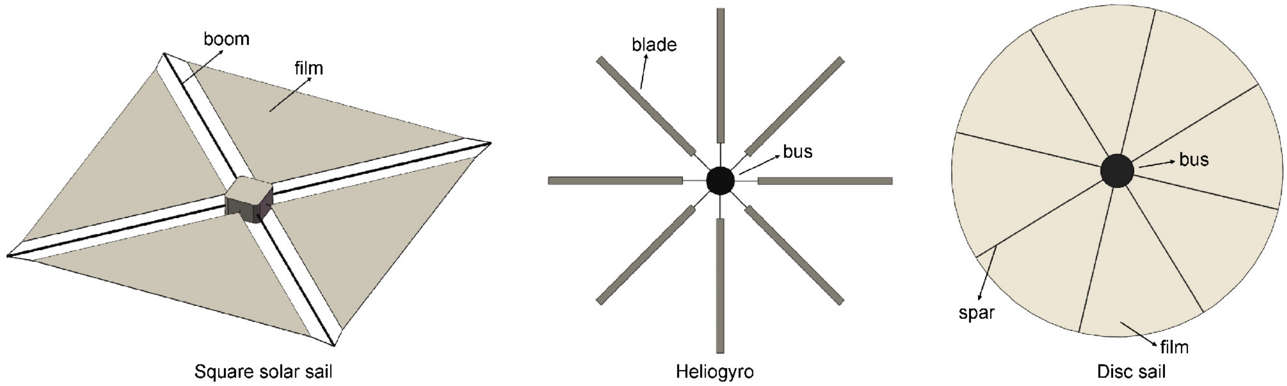

Fig. 13 Different sail configurations. Reproduced with permission from Ref. [173], © Choi, M., University of Toronto 2015.

the first vibration mode of the membrane and the model's validity was confirmed by numerical simulations using the multi-particle method. On the basis of Baddour's work [191], Zhang *et al.* [192] derived the analytical formula of the transverse nonlinear vibrations of a rotating flexible disk subjected to a rotating point force with a periodically varying rotating speed using Hamilton's principle. To explain the motion and behaviour of IKAROS in flight due to SRP, Tsuda *et al.* [193, 194] proposed a generalized spinning sail model that can be applied to realistic sails with non-flat surfaces and have non-uniform optical properties. This model considers the possible torques produced by SRP due to the static deformation of the sail membrane and the variation in the optical properties of the sail surface, and thus successfully reproduced the behaviours observed in the flight data. The linearized model was solved analytically and the stability and equilibrium of attitude motion were studied using this linearized model. In addition, the generalised spinning sail model also can be used to estimate the sail's actual shape [195], and to obtain the design criteria of the sail surface [196]. Besides the no-support sail, rare analytical flexible models of boom-support solar sails have been studied. Smith *et al.* [197] developed a two-dimensional model of a flexible solar sail representative of a kind of solar sail in which the sail and booms move synchronously for the lower modes. In this model, the mass of the sail membrane is simplified as distributed on two booms and the first asymmetric vibration mode of the booms is considered to couple with the angular motion. Using this analytical model, attitude control laws were designed and the results were evaluated against a finite element method. Recently, Fu proposed to shift the attachment point for attitude control [145]. The static equilibrium shape of the membrane subject to SRP should be determined to evaluate the SRP force and torque. Based on assumptions that the inextensible membrane is insusceptible to elastic deformation and has negligible bending resistance, and its steady-state shape is described by a surface of zero Gaussian curvature, the analytical static shape of the deformed membrane is obtained for different boundary conditions [198].

6.2 Numerical method

Finite element analysis method (FEAM) is useful for structural problems with complicated geometries, loadings, and material properties. In the past, many researchers have been trying to compute the dynamic responses of solar sail by using self-developed FEMs and nonlinear FEA softwares with special consideration of the peculiarity of a solar sail structure [217, 218, 220, 225, 231].

One of the challenges using FEM to deal with solar sail structural analysis lies in modeling the thin membrane. As mentioned above, one purpose for the dynamic analysis is to predict the global and local shape of the membrane to obtain accurate SRP force. Since the early 1970s, many studies have been conducted on the FEA of membranes. There are two categories of numerical analysis methods for predicting the shape of a tensioned membrane. One is using the tension filed (TF) method [199] to predict the global shape of the membrane. The other is using shell finite element to predict the shape of local wrinkles. The TF theory assumes that the membrane does not support compressive stress in a planer stress membrane. Most studies used the FEA based on the TF theory to study the wrinkling phenomenon by modifying the stress–strain relations, such as modified elasticity matrix that produces a uniaxial stress field [200], a penalty parameter modified material model [201–204]. These modification schemes have shortcomings including obscure physical meaning and losing nonlinearities originated from wrinkling. Due to these reasons, another approach based on modifying the deformation tensor instead of stress–strain relations is proposed [205, 206]. The method based on TF theory can be used in simulating the solar sail during deployment [207] and predicting the global shape of the membrane [208, 209] because the computation time is reasonable. However, studies based on the TF theory neglect the bending stiffness of the membrane and hence details of the wrinkles can't be obtained. Thus, FEMs based on shell elements are proposed to predict the local information of wrinkles. The shell elements considerate the negligibly small bending stiffness of membrane and the determination of wrinkle amplitudes. Miyamura [210] firstly used the linearized shell buckling technique to perform bifurcation analysis to predict wrinkling behavior. Wong and Pellegrino realized a similar analysis using the shear-deformable shell elements (S4R5) that are available in commercial FEM software ABAQUS [211]. Since then, the shell elements in the commercial software were widely used to predict wrinkles for membrane analysis. Comparison of the results with experiment measurements show that the shell finite elements in ABAQUS accurately predicted the shape and stiffness of the membrane [212]. However, the numerical stability and convergence is poor when above elements are incorporated into FEA to analyze the wrinkling membrane because of the dramatic variations of the local stiffness of the membrane and highly stiff differential equation. To overcome the obstacle, Pipkin *et al.* introduced the concept of relaxed strain-energy density to describe wrinkled state [213]. Wong and Pellegrino introduced the fictitious viscous forces to aid the convergence [214] Ding *et al.* presented a new membrane model with modified elasticity matrix to automatically characterize taut, wrinkled, and slackened states of membranes [215, 216]. The approach employs an optimization scheme instead of the iterative process to avoid convergence problems. The structural analysis problem of the membrane is well solved by the end of the twentieth century. Although these previous works mainly study small membranes, they provide a theoretical foundation of using FEA to analyze structural dynamics of a solar sail.

Conducting structural analysis at system-level of a large solar sail is still challenging because of the strong nonlinearity induced by the large thin sail membranes and very long and slender reinforcing booms, complex boundary conditions and loading conditions. Murphy firstly performed a dynamic structural analysis for sail sizes up to 300 m per edge with membrane elements using a FEAM [217]. Taleghani *et al.* employed shell finite element models in both the MSC/NASTRAN and ABAQUS commercial software programs to predict full-scale deformations and vibration modes of solar sail models up to 150 m in size [218]. Solar sail structural analysis usually has three steps for a non-spinning solar sail. The first step is pre-tensioning the membrane to get the out-of-plane stiffness in order to run the static analysis. A fictitious thermal load is commonly used to simulate the pre-tensioning by inducing contraction of the cables [208] Holland applies small out-of-plane forces in a quasi-random manner to force a feasible static configuration [219]. The second step is to apply the SRP load to perform another geometrically nonlinear static analysis. Since the membranes and booms are very flexible, the geometric elastic nonlinearity and the foreshortening effects have to be considered to model the nonlinear behavior [220]. A load incrementation scheme is usually used to aid the convergence. For the sail undergoing large overall motion during the deployment, Miyazaki *et al.* [221] proposed the stiffness reduction model (SRM) and Liu *et al.* [222] used the absolute nodal coordinate formulation to analyse the membrane systems. The energy momentum method (EMM) was applied to the SRM to guarantee the convergence in calculation [223]. If the wrinkling information is required, an eigenvalue buckling analysis is performed to predict the possible wrinkling modes of the membrane and then a post-wrinkling analysis is conducted [214]. The third step is to use the results of previous static analysis to perform the transient dynamic simulations. To obtain a correct solution using the FEM, one should apply boundary conditions correctly. Most previous simulations were conducted using the constrained boundary conditions. However, it was desired to model the response of the solar sails under a free-flying condition because the SRP load is balanced with inertial loads induced by a constant rigid body acceleration field. The structural analysis under a free-flying condition was performed by several authors [208, 224–226]. The results show that ignoring the inertial effects may induce boom deformations up to three times greater. Many studies have been performed to conduct structural analysis at system-level for structure and control designs. These studies include the scalable problems [217] and effects of the different connections between booms and membranes [208]. Choi and Damaren studied the coupling effects between the structure and control [227].

A full FEM formula is quite time-intensive for the design though it is high-fidelity. One way to solve this problem is to use a FEM reduction technique that balances the accuracy and efficiency of the FEM. Yamazaki *et al.* [228, 229] discussed a low-order model for the gossamer structure system by Empirical Model Reduction. The results showed that this low-order model is sufficiently accurate and may be applied to the practical design of a solar sail. Based on Sleight's high-fidelity FE model [208, 209], Smith *et al.* [197] proposed a reduced three-dimensional FE model for solar sail control via Guyan reduction [230]. The simulation results of this Guyan reduction were not verified in this paper, and it should be noted that the Guyan reduction completely ignores dynamics of slave degrees of freedom which leads to an overestimation of the natural frequencies. Li *et al.* [231] developed a more convincing three-dimensional solar sail model formulated in hybrid coordinates via the principle of virtual power for dynamics analysis and control design. This model was reduced by several pre-stressed modes obtained from the high-fidelity FE model and its accuracy was verified by the full FE model.

One reason for the FEA being time-consuming is the non-diagonal element stiffness matrix. During the design of IKAROS, multi-particle method (MPM) was prosed to simplify the membrane modeling by diagonalizing the element stiffness matrix. MPM is an approximated model in which the sail membranes are replaced simply by a network of lumped-masses and nonlinear springs that do not resist compressive forces. Miyazaki and Iwai [232] indicated that MPM can reproduce the dynamic responses of a membrane deployment predicted by finite-element analyses fairly accurately although it does not predict the stress distributions in a wrinkled membrane very accurately. Okuizumi *et al.* [233, 234] improved the MPM models by considering the buckling strength, crease stiffness, air drag and damping. He compared numerical simulations and experimental results of centrifugal deployments of hexagonal and square membranes with various fold patterns. The successful mission of IKAROS made it possible to validate MPM using actual flight data. Shirasawa *et al.* [235] compared the deployment response of the MPM and the actual flight. It was found that the MPM model could simulate the global behaviour of the membrane well, except for the damping of in-plane oscillation between the main body and the expanded membrane. In addition, they did an analysis on the differences between the observed shape in actual flight and simulated shape using MPM after IKAROS's successful deployment [236]. Part of the deformation phenomenon of the sail in the flight can be qualitatively explained by introducing some modifications into the MPM model. But some actual deformations failed to be explained by the MPM model so it is considered there were limitations in the analysis using the multi-particle model.

7 Outlook for future

Solar sails are a special class of spacecraft with a large gossamer structure. It is difficult to test the relevant technologies especially the dynamics and control technologies on ground because of its large size, along with vacuum and zero-gravity requirements. Therefore, high-fidelity simulations accompanied by ground or on-orbit experiments are important in the design of a solar sail mission. At present, several demonstration missions of solar sail technology, including IKAROS, NanoSailD, and Lightsail 1 have been flown. Some key technologies including deployment of large structures, attitude control of flexible solar sails using reflectivity control devices, and orbit manoeuvres using solar radiation pressure, have been tested on orbit. Therefore, more work has to be done to verify the scalability of these technologies.

The development trends of solar sails are similar to those of typical spacecraft. Large solar sails will accomplish certain unprecedented scientific objectives, usually constructed by national or international aerospace organizations. Small solar sails can be used to achieve some specific objectives at low cost and they can be built by commercial companies or even universities. A small solar sail is much easier and less expensive to build, and indeed CubeSat technology has enabled new advances in solar sail technology. An interesting new potential approach for validating and experimenting with novel solar sail designs and control laws is by the use of micro thin-film spacecraft as described by Johnson *et al.* [237]. Recently, a similar concept, termed "membrane spacecraft", is also proposed to envelop a piece of space debris in low Earth orbit [238]. These spacecraft are thin-film devices based on a polyimide or similar substrate, with avionics, instruments, photovoltaics, RCDs, and all the other components of a complete spacecraft bonded or printed on their surface. With masses of the order of milligrams to grams, targeting area to mass ratios of 10–20 g/m^2, the ability to pack hundreds of devices per CubeSat and divide a single low cost CubeSat mission between dozens or even hundreds of such spacecraft can drive the cost and risk of on orbit verification of ideas down to within the reach of even individual students.

Acknowledgements

This work was supported by the National Natural Science Foundation of China (Grant No. 117722167 and 11822205).

References

[1] Zander's. Problems of flight by jet propulsion: Interplanetary flights, was translated by NASA. See NASA Technical Translation F-147 (1964); specifically, Section 7: Flight Around a Planet's Satellite for Accelerating or Decelerating Spaceship, **1925**, 290–292.

[2] Prince, J. L. H., Powell, R. W., Murri, D. Autonomous aerobraking: A design, development, and feasibility study. AAS 11-473, NASA Langley Research Center, **2011**.

[3] Available at: https://spaceflightsystems.grc.nasa.gov/SSPO/FactSheets/ACAP%20Fact%20Sheet.pdf.

[4] Janhunen, P. Electric sail for spacecraft propulsion. *Journal of Propulsion and Power*, **2004**, 20(4): 763–764.

[5] Zubrin, R. M., Andrews, D. G. Magnetic sails and interplanetary travel. *Journal of Spacecraft and Rockets*, **1991**, 28(2): 197–203.

[6] Maxwell, J. C. A treatise on electricity and magnetism, Clarendon Press, **1873**.

[7] Lebedew, P. The physical causes of the deviations from Newton's law of gravitation. *Astrophysical Journal*, **1902**, 16: 155–161.

[8] Nichols, E. F., Hull, G. F. A preliminary communication on the pressure of heat and light radiation. *Physics Review (Series I)*, **1901**, 13(5): 307–320.

[9] Nichols, E. F., Hull, G. F. The pressure due to radiation. *Astrophysical Journal*, **1903**, 17: 315.

[10] Tsiolkovsky, K. E. Extension of man into outer space. In: Proceedings of Symposium Jet Propulsion No.2, **1936**.

[11] Tsander, K. From a scientific heritage. NASA Technical Translation No. TTF-541, NASA, **1967**.

[12] Tsiolkovsky, K. E. Exploration of the universe with reaction machines. *The Science Review*, **1903**(5).

[13] Oberth, H. Die rakete zu den planetenräumen, R. Oldenbourg, **1923**, 86–88.

[14] Oberth, H. Wege zur raumschiffahrt. R. Oldenbourg, **1929**, 353–371.

[15] Wiley, C. (Pseudonym: Sanders, R.), 'Clipper ships of space'. *Astounding Science Fiction*, **1951**, 136–143.

[16] MacNeal, R. H. Comparison of the solar sail with electric propulsion systems. NASA CR-1986, National Aeronautics and Space Administration, **1972**.

[17] McInnes, C. R. Solar sail mission applications for non-Keplerian orbits. *Acta Astronautica*, **1999**, 45(4–9): 567–575.

[18] Sohn, R. L. Attitude stabilization by means of solar radiation pressure. *ARS Journal*, **1959**, 29(5): 371–373.

[19] Renner, U. Attitude control by solar sailing-a promising experiment with OTS-2. *European Space Agency Journal*, **1979**, 3: 35–40.

[20] Modi, V. J. On the semi-passive attitude control and propulsion of space vehicles using solar radiation pressure. *Acta Astronautica*, **1995**, 35(2–3): 231–246.

[21] Acord, J. D., Nicklas, J. C. Theoretical and practical aspects of solar pressure attitude control for interplanetary spacecraft. In: Proceedings of Guidance and Control Conference, **1964**, 73–101.

[22] Shirley, D. L. The mariner 10 mission to Venus and mercury. In: Proceedings of the New Face of Space Selected Proceedings of the 53rd International Astronautical Federation Congress, **2002**.

[23] O'Shaughnessy, D. J., McAdams, J. V., Williams, K. E., Page, B. R. Fire sail: Messenger's use of solar radiation pressure for accurate mercury flybys. AAS 09–014, **2009**.

[24] David, J. Sailing to the world's most famous comet. Story of Lightsail-Part 1. Available at: http://sail.planetary.org/story-part-1.html.

[25] Znamya (satellite). Available at: https://en.wikipedia.org/wiki/Znamya (satellite).

[26] Alexander, A. Japanese researchers successfully test unfurling of solar sail on rocket flight. Planetary News, 2004-08-10.

[27] Lovgren, S. Solar sail spacecraft set for launch. National Geographic News, 2005-06-20.

[28] Leipold, M., Eiden, M., Garner, C. E., Herbeck, L., Kassing, D., Niederstadt, T., Krüger, T., Pagel, G., Rezazad, M., Rozemeijer, H. et al. Solar sail technology development and demonstration. In: Selected Proceedings of the 4th IAA International Conference on Low Cost Planetary Missions, **2003**.

[29] Seboldt, W., Leipold, M., Rezazad, M., Herbeck, L., Unkenbold, W., Kassing, D., Eiden, M. Ground-based demonstration of solar sail technology. In: Proceedings of the 51st International Astronautical Congress, **2000**.

[30] Seefeldt, P. A stowing and deployment strategy for large membrane space systems on the example of Gossamer-1. *Advances in Space Research*, **2017**, 60(6): 1345–1362.

[31] Seefeldt, P., Spietz, P., Sproewitz, T., Grundmann, J. T., Hillebrandt, M., Hobbie, C., Ruffer, M., Straubel, M., Tóth, N., Zander, M. Gossamer-1: Mission concept and technology for a controlled deployment of gossamer spacecraft. *Advances in Space Research*, **2017**, 59(1): 434–456.

[32] Dachwald, B., Boehnhardt, H., Broj, U., Geppert, U. R. M. E., Grundmann, J. T., Seboldt, W., Seefeldt, P., Spietz, P., Johnson, L., Kührt, E. et al. Gossamer roadmap technology reference study for a multiple NEO rendezvous mission. *Advances in Solar Sailing*, **2014**.

[33] Peloni, A., Ceriotti, M., Dachwald, B. Solar-sail trajectory design for a multiple near-earth-asteroid rendezvous mission. *Journal of Guidance, Control, and Dynamics*, **2016**, 39(12): 2712–2724.

[34] West, J. L., Derbès, B. Solar sail vehicle system design for the geostorm warning mission. In: Proceedings of the AIAA Space 2000 Conference and Exposition, **2000**.

[35] Price, H., Ayon, J., Garner, C., Klose, G., Mettler, E., Sprague, G. Design for a solar sail demonstration mission. In: Proceedings of Space Technology and Applications International Forum, **2001**.

[36] Murphy, D. M., Murphey, T. W., Gierow, P. A. Scalable solar sail subsystem design considerations. In: Proceedings of the 43rd AIAA/ASME/ASCE/AHS/ASC Structures, Structural Dynamics, and Materials Conference, **2002**.

[37] Garner, C., Diedrich, B., Leipold, M. A summary of solar sail technology developments and proposed demonstration missions. In: Proceedings of the 35th Joint Propulsion Conference and Exhibit, **1999**.

[38] Whorton, M., Heaton, A., Pinson, R., Laue, G., Adams, C. L. NanoSail-D: The first flight demonstration of solar sails for nanosatellites. In: Proceedings of the 22nd Annual AIAA/USU Conference on Small Satellites, **2008**.

[39] Johnson, L., Young, R., Montgomery, E., Alhorn, D. Status of solar sail technology within NASA. In: Proceedings of the 2nd International Symposium on Solar Sailing, **2010**.

[40] NASA's first solar sail NanoSail-D deploys in low-Earth orbit. NASA, Small Satellite Missions. Available at: https://www.nasa.gov/mission_pages/smallsats/11-010.html.

[41] Wall, M. World's largest solar sail to launch in November 2014. Available at: http://www.space.com/21556-sunjammer-solar-sail-launch-2014.html.

[42] McNutt, L., Johnson, L., Clardy, D., Castillo-Rogez, J., Frick, A., Jones, L. Near-earth asteroid scout. Available at: https://ntrs.nasa.gov/archive/nasa/casi.ntrs.nasa.gov/20140012882.pdf.

[43] NEA-Scout, Gunter's Space Page. Available at: http://space.skyrocket.de/doc_sdat/nea-scout.htm.

[44] Mori, O., Sawada, H., Funase, R., Morimoto, M., Endo, T., Yamamoto, T., Tsuda, Y., Kawakatsu, Y., Kawaguchi, J. IKAROS demonstration team and solar sail working group, first solar power sail demonstration by IKAROS. In: Proceedings of the 27th International Symposium on Space Technology and Science, **2009**.

[45] Okada, T., Kebukawa, Y., Aoki, J., Matsumoto, J., Yano, H., Iwata, T., Mori, O., Bibring, J. P., Ulamec, S., Jaumann R. et al. Science exploration and instrumentation of the OKEANOS mission to a Jupiter Trojan asteroid using the solar power sail. *Planetary and Space Science*, **2018**, 161: 99–106.

[46] LightSail: A solar sailing spacecraft from the planetary society. Available at: http://sail.planetary.org/.

[47] DeOrbitSail (DOS) Nanosatellite mission. Available at: https://directory.eoportal.org/web/eoportal/satellite-missions/d/deorbitsail.

[48] Trofimov, S. P., Ovchinnikov, M. Y. Performance scalability of square solar sails. *Journal of Spacecraft and Rockets*, **2018**, 55(1): 242–246.

[49] Derbes, B., Veal, G., Rogan, J., Chafer, C. Team encounter solar sails. In: Proceedings of the 45th AIAA/ASME/ASCE/AHS/ASC Structures, Structural Dynamics & Materials Conference, **2004**.

[50] Johnson, L., Young, R., Montgomery, E., Alhorn, D. Status of solar sail technology within NASA. *Advances in Space Research*, **2011**, 48(11): 1687–1694.

[51] Zhang, M., Fang, S. L., Zakhidov, A. A., Lee, S. B., Aliev, A. E., Williams, C. D., Atkinson, K. R., Baughman, R. H. Strong, transparent, multifunctional, carbon nanotube sheets. *Science*, **2005**, 309(5738): 1215–1219.

[52] Drexler, K. E. Design of a high performance solar sail system. Master Dissertation, Massachusetts Institute of Technology, Massachusetts, USA, **1977**.

[53] Young, R. M., Montgomery, E. E., Adams, C. L. TRL assessment of solar sail technology development following the 20-meter system ground demonstrator hardware testing. In: Proceedings of the 48th AIAA/ASME/ASCE/AHS/ASC Structures, Structural Dynamics, and Materials Conference, **2007**.

[54] Grundmann, J. T., Bauer, W., Biele, J., Boden, R., Ceriotti, M., Cordero, F., Dachwald, B., Dumont, E., Grimm, C. D., Herčík, D. et al. Capabilities of Gossamer-1 derived small spacecraft solar sails carrying MASCOT-derived nanolanders for in-situ surveying of NEAs. *Acta Astronautica*, in press, DOI: 10.1016/J.ACTAASTRO.2018.03.019.

[55] Garwin, R. Solar sailing: A practical method of propulsion within the solar system. *Jet Propulsion*, **1958**, 28(123): 188–190.

[56] Tsu, T. C. Interplanetary travel by solar sail. *ARS Journal*, **1959**, 29(6): 422–427.

[57] London, H. S. Some exact solutions of the equations of motion of a solar sail with constant sail setting. *Journal of the American Rocket Society*, **1960**, 30: 198–200.

[58] van der Ha, J. C., Modi, V. J. Long-term evaluation of three-dimensional heliocentric solar sail trajectories with arbitrary fixed sail setting. *Celestial Mechanics*, **1979**, 19(2): 113–138.

[59] Pontryagin, L. S., Boltyanskii, V. G., Gamkrelidze, R. V., Mishechenko, E. F. The mathematical theory of optimal processes, Wiley, **1962**.

[60] Macdonald, M., McInnes, C. R. Analytical control laws for planet-centered solar sailing. *Journal of Guidance, Control, and Dynamics*, **2005**, 28(5): 1038–1048.

[61] Coverstone, V. L., Prussing J. E. Technique for escape from geosynchronous transfer orbit using a solar sail. *Journal of Guidance, Control, and Dynamics*, **2003**, 26(4): 628–634.

[62] Kim, M. Continuous low-thrust trajectory optimization: Techniques and applications. Master Dissertation, Virginia Polytechnic Institute and State University, Virginia, USA, **2005**.

[63] Gong, S. P., Gao, Y. F., Li, J. F. Solar sail time-optimal interplanetary transfer trajectory design. *Research in Astronomy and Astrophysics*, **2011**, 11(8): 981–996.

[64] Garg, D., Patterson, M. A., Francolin, C., Darby, C. L., Huntington, G. T., Hager, W. W., Rao, A. V. Direct trajectory optimization and costate estimation of finite-horizon and infinite-horizon optimal control problems using a Radau pseudospectral method. *Computational Optimization and Applications*, **2011**, 49(2): 335–358.

[65] Zhukov, A. N., Lebedev, V. N. Variational problem of transfer between heliocentric circular orbits by means of a solar sail. *Cosmic Research*, **1964**, 2: 41–44.

[66] Sauer, C. G. Jr. Optimum solar-sail interplanetary trajectories. In: Proceedings of Astrodynamics Conference, **1976**.

[67] Sauer, C. G. Jr. A comparison of solar sail and ion drive trajectories for a Halley's comet rendezvous mission. AAS Paper 77–104, **1977**.

[68] Colasurdo, G., Casalino, L. Optimal control law for interplanetary trajectories with nonideal solar sail. *Journal of Spacecraft and Rockets*, **2003**, 40(2): 260–265.

[69] SubbaRao, P. V., Ramanan, R. V. Optimal three-dimensional heliocentric solar-sail rendezvous transfer trajectories. *Acta Astronautica*, **1993**, 29(5): 341–345.

[70] Quarta, A. A., Mengal, G. Solar sail missions to mercury with Venus gravity assist. *Acta Astronautica*, **2009**, 65(3–4): 495–506.

[71] Otten, M., McInnes, C. R. Near minimum-time trajectories for solar sails. *Journal of Guidance, Control, and Dynamics*, **2001**, 24(3): 632–634.

[72] Mengali, G., Quarta, A. A. Solar sail trajectories with piecewise-constant steering laws. *Aerospace Science and Technology*, **2009**, 13(8): 431–441.

[73] Macdonald, M., McInnes, C. R., Dachwald, B. Heliocentric solar sail orbit transfers with locally optimal control laws. *Journal of Spacecraft and Rockets*, **2007**, 44(1): 273–276.

[74] Hokamoto, S., Sachimoto, K., Fujita, K. Trajectory design of solar sail spacecraft for interplanetary rendezvous missions. *Transactions of Space Technology Japan*, **2009**, 7(26): 37–42.

[75] NASA Office of Space Science. Sun-earth connection roadmap: Strategic planning for the years 2000–2020. NASA, **1997**.

[76] Macdonald, M., Hughes, G. W., McInnes, C. R., Lyngvi, A., Falkner, P., Atzei, A. Solar polar orbiter: A solar sail technology reference study. *Journal of Spacecraft and Rockets*, **2006**, 43(5): 960–972.

[77] Goldstein, B. E., Buffington, A., Cummings, A. C., Fisher, R. R., Jackson, B. V., Liewer, P. C., Mewaldt, R. A., Neugebauer, M. Solar polar sail mission: Report of a study to put a scientific spacecraft in a circular polar orbit about the Sun. In: Proceedings of the SPIE 3442, International Symposium on Optical Science, Engineering, and Instrumentation, **1998**.

[78] Sauer, C. G. Jr. Solar sail trajectories for solar-polar and interstellar probe missions. In: Proceedings of the AAS/AIAA Astrodynamics Specialists Conference, **1999**.

[79] Dachwald, B., Ohndorf, A., Wie, B. Solar sail trajectory optimization for the Solar Polar Imager (SPI) Mission. In: Proceedings of the AIAA/AAS Astrody-namics Specialist Conference and Exhibit, **2006**.

[80] Mengali, G., Quarta, A. A. Solar sail near-optimal circular transfers with plane change. *Journal of Guidance, Control, and Dynamics*, **2009**, 32(2): 456–463.

[81] Macdonald, M. Analytical, circle-to-circle low-thrust transfer trajectories with plane change. In: Proceedings of AIAA Guidance, Navigation, and Control (GNC) Conference, **2013**.

[82] Driver, J. M. Analysis of an arctic polesitter. *Journal of Spacecraft and Rockets*, **1980**, 17(3): 263–269.

[83] McInnes, C. R., Simmons, J. F. L. Solar sail halo orbits part II-geocentric case. *Journal of Spacecraft and Rockets*, **1992**, 29(4): 472–479.

[84] Hughes, G. W., McInnes, C. R. Solar sail hybrid trajectory optimization for non-Keplerian orbit transfers. *Journal of Guidance, Control, and Dynamics*, **2002**, 25(3): 602–604.

[85] Ceriotti, M., Heiligers, J., McInnes. C. R. Trajectory and spacecraft design for a pole-sitter mission. *Journal of Spacecraft and Rockets*, **2014**, 51(1): 311–326.

[86] Heiligers, J., Ceriotti, M., McInnes. C. R., Biggs, J. D. Mission analysis and systems design of a near-term and far-term pole-sitter mission. *Acta Astronautica*, **2014**, 94(1): 455–469.

[87] West, J. The Geostorm Warning Mission: enhanced opportunities based on new technology. In: Proceedings of the 14th AAS/AIAA Space Flight Mechanics Conference, **2004**.

[88] McInnes, C. Solar sailing: Technology, dynamics and mission applications, Springer, **1999**.

[89] Lisano, M., Lawrence, D., Piggott, S. Solar sail transfer trajectory design and stationkeeping control for missions to the Sub-L1 equilibrium region. In: Proceedings of the 15th AAS/AIAA Spaceflight Mechanics Conference, **2005**.

[90] Koon, W. S., Lo, M. W., Marsden, J. E., Ross, S. D. Heteroclinic connections between periodic orbits and resonance transitions in celestial mechanics. *Chaos*, **2000**, 10(2): 427–469.

[91] Biggs, J. D., Waters, T., McInnes, C. New periodic orbits in the solar sail three-body problem. *Nonlinear Science and Complexity*, **2011**.

[92] Gong, S. P., Baoyin, H. X., Li, J. F. Solar sail three-body transfer trajectory design. *Journal of Guidance, Control, and Dynamics*, **2010**, 33(3): 873–886.

[93] Gong, S. P., Li, J. F., Baoyin, H. X. Solar sail transfer trajectory from L1 point to sub-L1 point. *Aerospace Science and Technology*, **2011**, 15(7): 544–554.

[94] Wallace, R. A. Precursor missions to interstellar exploration. In: Proceedings of the 1999 IEEE Aerospace Conference, **1999**.

[95] Johnson, L., Leifer, S. Propulsion options for interstellar exploration. In: Proceedings of the 36th AIAA/ASME/SAE/ASEE Joint Propulsion Conference and Exhibit, **2000**.

[96] Wallace, R. A., Ayon, J. A., Sprague, G. A. Interstellar probe mission/system concept. In: Proceedings of 2000 IEEE Aerospace Conference, **2000**.

[97] Nieto, M. M., Turyshev, S. G. Measuring the interplanetary medium with a solar sail. *International Journal of Modern Physics D*, **2004**, 13(5): 899–906.

[98] Garner, C. E., Layman, W., Gavit, S. A., Knowles, T. A solar sail design for a mission to the near-interstellar medium. *AIP Conference Proceedings*, **2000**, 504: 947–961.

[99] Dachwald, B. Optimal solar-sail trajectories for missions to the outer solar system. *Journal of Guidance, Control, and Dynamics*, **2005**, 28(6): 1187–1193.

[100] Lyngvi, A., Falkner, P., Peacock, A. The interstellar heliopause probe, Tools and Technologies for Future Planetary Exploration. In: Proceedings of the 37th ESLAB Symposium, **2004**.

[101] Lyngvi, A., Falkner, P., Kemble, S., Leipold, M., Peacock, A. The interstellar heliopause probe. *Acta Astronautica*, **2005**, 57(2–8): 104–111.

[102] Lyngvi, A., Falkner, P., Peacock, A. The interstellar heliopause probe technology reference study. *Advances in Space Research*, **2005**, 35(12): 2073–2077.

[103] Leipold, M., Fichtner, H., Heber, B., Groepper, P., Lascar, S., Burger, F., Eiden, M., Niederstadt, T., Sickinger, C., Herbeck, L. et al. Heliopause explorer—a sailcraft mission to the outer boundaries of the solar system. *Acta Astronautica*, **2006**, 59(8–11): 785–796.

[104] Macdonald, M., McInnes, C., Hughes, G. Technology requirements of exploration beyond Neptune by solar sail propulsion. *Journal of Spacecraft and Rockets*, **2010**, 47(3): 472–483.

[105] Sharma, D. N., Scheeres, D. J. Solar system escape trajectories using solar sails. *Journal of Spacecraft and Rockets*, **2004**, 41(4): 684–687.

[106] Dachwald, B., Seboldt, W., Macdonald, M., Mengali, G., Quarta, A. A., McInnes, C. R., Rios-Reyes, L., Scheeres, D. J., Wie, B., Görlich, M. et al. Potential solar sail degradation effects on trajectory and attitude control. In: Proceedings of AIAA Guidance, Navigation, and Control Conference and Exhibit, **2005**.

[107] Sznajder, M., Geppert, U., Dudek, M. Degradation of metallic surfaces under space conditions, with particular emphasis on Hydrogen recombination processes. *Advances in Space Research*, **2015**, 56(1): 71–84.

[108] He, J., Gong, S. P., Jiang, F. H., Li, J. F. Time-optimal rendezvous transfer trajectory for restricted cone-angle range solar sails. *Acta Mechanica Sinica*, **2014**, 30(5): 628–635.

[109] McKay, R. J., Macdonald, M., Biggs, J., McInnes, C. Survey of highly non-Keplerian orbits with low-thrust propulsion. *Journal of Guidance, Control, and Dynamics*, **2011**, 34(3): 645–666.

[110] Leipold, M., Borg, E., Lingner, S., Pabsch, A., Sachs, R., Seboldt, W. Mercury orbiter with a solar sail spacecraft. *Acta Astronautica, 1995*, 35(S1): 635–644.

[111] McInnes, C. R., Macdonald, M., Angelopolous, V., Alexander, D. GEOSAIL: Exploring the geomagnetic tail using a small solar sail. *Journal of Spacecraft and Rockets*, **2001**, 38(4): 622–629.

[112] Macdonald, M., Hughes, G. W., McInnes, C., Lyngvi, A., Falkner, P., Atzei, A. GeoSail: An elegant solar sail demonstration mission. *Journal of Spacecraft and Rockets*, **2007**, 44(4): 784–796.

[113] Gong, S. P., Li, J. F., Baoyin, H. X., Simo, J. A new solar sail orbit. *Science China Technological Sciences*, **2012**, 55(3): 848–855.

[114] Tresaco, E., Elipe, A., Carvalho, J. P. S. Frozen orbits for a solar sail around Mercury. *Journal of Guidance, Control, and Dynamics*, **2016**, 39(7): 1659–1666.

[115] Baoyin, H. X., McInnes, C. R. Solar sail equilibria in the elliptical restricted three-body problem. *Journal of Guidance, Control, and Dynamics*, **2006**, 29(3): 538–543.

[116] Funase, R., Shirasawa, Y., Mimasu, Y., Mori, O., Tsuda, Y., Saiki, T., Kawaguchi, J. On-orbit verification of fuel-free attitude control system for spinning solar sail utilizing solar radiation pressure. *Advances in Space Research*, **2011**, 48(11): 1740–1746.

[117] Gong, S. P., Li, J. F. Solar sail halo orbit control using reflectivity control devices. *Transactions of the Japan Society for Aeronautical and Space Sciences*, **2014**, 57(5): 279–288.

[118] Mu, J. S., Gong, S. P., Li, J. F. Reflectivity-controlled solar sail formation flying for magnetosphere mission. *Aerospace Science and Technology*, **2013**, 30(1): 339–348.

[119] Mu, J. S., Gong, S. P., Li, J. F. Coupled control of reflectivity modulated solar sail for GeoSail formation flying. *Journal of Guidance, Control, and Dynamics*, **2015**, 38(4): 740–751.

[120] Gong, S. P., Li, J. F. Solar sail heliocentric elliptic displaced orbits. *Journal of Guidance, Control, and Dynamics*, **2014**, 37(6): 2021–2026.

[121] Aliasi, G., Mengali, G., Quarta, A. A. Artificial Lagrange points for solar sail with electrochromic material panels. *Journal of Guidance, Control, and Dynamics*, **2013**, 36(5): 1544–1550.

[122] Gong, S. P., Li, J. F. Equilibria near asteroids for solar sails with reflection control devices. *Astrophysics and Space Science*, **2015**, 355(2): 213–223.

[123] Baoyin, H. X., Mcinnes, C. R. Solar sail halo orbits at the Sun–Earth artificial L_1 point. *Celestial Mechanics and Dynamical Astronomy*, **2006**, 94(2): 155–171.

[124] Biggs, J. D., McInnes, C. R., Waters, T. Control of solar sail periodic orbits in the elliptic three-body problem. *Journal of Guidance, Control, and Dynamics*, **2009**, 32(1): 318–320.

[125] Gong, S. P., Li, J. F. Solar sail periodic orbits in the elliptic restricted three-body problem. *Celestial Mechanics and Dynamical Astronomy*, **2015**, 121(2): 121–137.

[126] Vulpetti, G. Missions to the heliopause and beyond by staged propulsion spacecrafts. In: Proceedings of the 43rd World Space Congress, **1992**.

[127] Vulpetti, G. 3D high-speed escape heliocentric trajectories by all-metallic-sail low-mass sailcraft. *Acta Astronautica*, **1996**, 39(1–4): 161–170.

[128] Vulpetti, G. Sailcraft at high speed by orbital angular momentum reversal. *Acta Astronautica*, **1997**, 40(10): 733–758.

[129] Sauer, C. Solar sail trajectories for solar polar and interstellar probe missions. In: Proceedings of the AAS/AIAA Astrodynamics Specialist Conference, **1999**.

[130] Zeng, X. Y., Baoyin, H. X., Li, J. F., Gong, S. P. Feasibility analysis of the angular momentum reversal trajectory via hodograph method for high performance solar sails. *Science China Technological Sciences*, **2011**, 54(11): 2951–2957.

[131] Mengali, G., Quarta, A. A., Romagnoli, D., Circi, C. H^2-reversal trajectory: A new mission application for high-performance solar sails. *Advances in Space Research*, **2011**, 48(11): 1763–1777.

[132] Zeng, X. Y., Baoyin, H. X., Li, J. F., Gong, S. P. New applications of the H-reversal trajectory using solar sails. *Research in Astronomy and Astrophysics*, **2011**, 11(7): 863–878.

[133] Gong, S. P., Li, J. F., Zeng, X. Y. Utilization of an H-reversal trajectory of a solar sail for asteroid deflection. *Research in Astronomy and Astrophysics*, **2011**, 11(10): 1123–1133.

[134] Šuvakov, M., Dmitrašinović, V. Three classes of Newtonian three-body planar periodic orbits. *Physical Review Letters*, **2013**, 110(11): 114301.

[135] Hamilton, D. P. Fresh solutions to the four-body problem. *Nature*, **2016**, 533(7602): 187–188.

[136] Wie, B. Solar sail attitude control and dynamics, Part 1. *Journal of Guidance, Control, and Dynamics*, **2004**, 27(4): 526–535.

[137] Wie, B. Solar sail attitude control and dynamics, Part 2. *Journal of Guidance, Control, and Dynamics*, **2004**, 27(4): 536–544.

[138] Steyn, W. H. Attitude control actuators, sensors and algorithms for a solar sail Cubesat. In: Proceedings of the 62nd International Astronautical Congress, **2011**.

[139] Jordaan, H. W., Steyn, W. H. The attitude control of a tri-spin solar sail satellite. *Advances in Solar Sailing*, **2014**, 755–769.

[140] Polites, M., Kalmanson, J., Mangus, D. Solar sail attitude control using small reaction wheels and magnetic torquers. *Proceedings of the Institution of Mechanical Engineers, Part G: Journal of Aerospace Engineering*, **2008**, 222(1): 53–62.

[141] Wie, B., Murphy, D., Paluszek, M., Thomas, S. Robust attitude control systems design for solar sails, Part 2: MicroPPT-based secondary ACS. In: Proceedings of the AIAA Guidance, Navigation, and Control Conference and Exhibit, **2004**.

[142] Lawrence, D. A., Piggott, S. W. Integrated trajectory and attitude control for a four-vane solar sail. In: Proceedings of the AIAA Guidance, Navigation, and Control Conference and Exhibit, **2005**.

[143] Mettler, E., Açıkme, A. B., Ploen, S. R. Attitude dynamics and control of solar sails with articulated vanes. In: Proceedings of the AIAA Guidance, Navigation, and Control Conference and Exhibit, **2005**.

[144] Fu, B., Eke, F. O. An attitude control methodology for large solar sails. In: Proceedings of the AIAA Guidance, Navigation, and Control (GNC) Conference, **2013**.

[145] Fu, B., Eke, F. O. A reorientation scheme for large solar sails. *Advances in the Astronautical Sciences*, **2014**, 150: 623–638.

[146] Funase, R., Kanno, G., Tsuda, Y. Controllability of propellant-free attitude control system for spinning solar sail using thin-film reflectivity control devices considering arbitrary sail deformation. In: Proceedings of the 63rd International Astronautical Congress, **2012**.

[147] Funase, R., Kanno, G., Tsuda, Y. Modeling and on-orbit performance evaluation of propellant-free attitude control system for spinning solar sail via optical parameter switching. In: Proceedings of the AAS/AIAA Astrodynamics Specialists Conference, **2012**, 1737–1754.

[148] Guerrant, D. V., Wilkie, W. K., Lawrence, D. A. Heliogyro blade twist control via reflectivity modulation. In: Proceedings of the 53rd AIAA/ASME/ASCE/AHS/ASC Structures, Structural Dynamics and Materials Conference, **2012**.

[149] Borggräfe, A., Heiligers, J., Ceriotti, M., McInnes, C.R. Optical control of solar sails using distributed reflectivity. In: Proceedings of the Spacecraft Structures Conference, **2014**.

[150] Benjamin, L. D. Attitude control and dynamics of solar sails. Master Dissertation, University of Washington, Washington, USA, **2001**.

[151] Wie, B., Thomas, S., Paluszek, M., Murphy, D. Propellantless AOCS design for a 160-m, 450-kg sailcraft of the Solar Polar Imager Mission. In: Proceedings of the 41st AIAA/ASME/SAE/ASEE Joint Propulsion Conference & Exhibit, **2005**.

[152] Wie, B., Murphy, D. Solar-sail attitude control design for a sail flight validation mission. *Journal of Spacecraft and Rockets*, **2007**, 44(4): 809–821.

[153] Bolle, A., Circi, C. Solar sail attitude control through in-plane moving masses. *Journal of Aerospace Engineering*, **2008**, 222(1): 81–94.

[154] Scholz, C., Romagnoli, D., Dachwald, B. Performance analysis of an attitude control system for solar sails using sliding masses. In: Proceedings of the Second International Symposium on Solar Sailing, **2010**.

[155] Romagnoli, D., Oehlschlagel, T. High performance two degrees of freedom attitude control for solar sails. *Advances in Space Research*, **2011**, 48(11): 1869–1879.

[156] Seboldt, W., Dachwald, B. Solar sails for near-term advanced scientific deep space missions. In: Proceedings of the 8th International Workshop on Combustion and Propulsion, **2002**.

[157] Fu, B., Sperber, E., Eke, F. Solar sail technology—A state of the art review. *Progress in Aerospace Sciences*, **2016**, 86: 1–19.

[158] Nasir, N. S., Theodorou, T., Lappas, V. J. Ground demonstration of a solar sail attitude control actuator. In: Proceedings of the AIAA Guidance, Navigation, and Control Conference, **2010**.

[159] Adeli, S. N., Lappas, V. J., Wie, B. A scalable bus-based attitude control system for Solar Sails. *Advances in Space Research*, **2011**, 48(11): 1836–1847.

[160] Steyn, W. H., Lappas, V. Cubesat solar sail 3-axis stabilization using panel translation and magnetic torquing. *Aerospace Science and Technology*, **2011**, 15(6): 476–485.

[161] Acord, J. D., Nicklas, J. C. Theoretical and practical aspects of solar pressure attitude control for interplanetary spacecraft. *Guidance and Control*, **1964**, 73–91.

[162] Polyakhova, E. Space flight using a solar sail—the problems and the prospects. Kosmicheskiy Polet Solnechnym Parusom, Moscow, **1986**.

[163] Kirpichnikov, S. N., Kirpichnikova, E. S., Polyakhova, E. N., Shmyrov, A. S. Planar heliocentric roto-translatory motion of a spacecraft with a solar sail of complex shape. *Celestial Mechanics and Dynamical Astronomy*, **1995**, 63(3–4): 255–269.

[164] van de Kolk, C. B., Flandro, G. A. Solar sail passive attitude stability and control. *AIP Conference Proceedings*, **2001**, 552: 373–378.

[165] Atchison, J. A., Peck, M. A. A passive, sun-pointing, millimeter-scale solar sail. *Acta Astronautica*, **2010**, 67(1–2): 108–121.

[166] McInnes, C. R. Passive control of displaced solar sail orbits. *Journal of Guidance, Control, and Dynamics*, **1998**, 21(6): 975–982.

[167] Gong, S. P., Li, J. F., Baoyin, H. X. Passive stability design for solar sail on displaced orbits. *Journal of Spacecraft and Rockets*, **2007**, 44(5): 1071–1080.

[168] Gong, S. P., Li, J. F., Zhu, K. J. Dynamical analysis of a spinning solar sail. *Advances in Space Research*, **2011**, 48(11): 1797–1809.

[169] Gong, S. P., Li J. F. Spin-stabilized solar sail for displaced solar orbits. *Aerospace Science and Technology*, **2014**, 32(1): 188–199.

[170] Kreissl, S., Sakamoto, H., Park, K. C., Baier, H. Design improvements of a solar sail for stiffness increase and passive attitude stabilization. In: Proceedings of the 48th AIAA/ASME/ASCE/AHS/ASC Structures, Structural Dynamics, and Materials Conference, **2007**.

[171] Hu, X. S., Gong, S. P., Li, J. F. Attitude stability criteria of axisymmetric solar sail. *Advances in Space Research*, **2014**, 54(1): 72–81.

[172] Gong, S. P., Li, J. F. A new inclination cranking method for a flexible spinning solar sail. *IEEE Transactions on Aerospace and Electronic Systems*, **2015**, 51(4): 2680–2696.

[173] Choi, M. Flexible dynamics and attitude control of a square solar sail. Ph.D. Dissertation, University of Toronto, Toronto, Canada, **2015**.

[174] Wilkie, W. K., Warren, J. E., Horta, L. G., Lyle, K. H., Juang, J. N., Gibbs, S. C., Dowell, E. H., Guerrant, D. V., Lawrence, D. A. Recent advances in heliogyro solar sail structural dynamics, stability, and control research. In: Proceedings of the 2nd AIAA Spacecraft Structures Conference, **2015**.

[175] Fedor, J. V. Analytical theory of the stretch Yo-Yo for de-spin of satellites. NASA TN D-1676, National Aeronautics and Space Administration, **1963**.

[176] Collins, R. L. A three-dimensional analysis of a tangential Yo-Yo despin device on a rotating body. NASA TN D-3848, National Aeronautics and Space Administration, **1967**.

[177] Gärdsback, M. Deployment control of spinning space webs and membranes. SE-100 44, Royal Institute of Technology, **2008**.

[178] Gärdsback, M., Tibert, G. Deployment control of spinning space Webs. *Journal of Guidance, Control, and Dynamics*, **2009**, 32(1): 40–50.

[179] Gärdsback, M., Tibert, G. Optimal deployment control of spinning space webs and membranes. *Journal of Guidance, Control, and Dynamics*, **2009**, 32(5): 1519–1530.

[180] Haraguchi, D., Sakamoto, H., Shirasawa, Y., Mori, O. Design criteria for spin deployment of gossamer structures considering nutation dynamics. In: Proceedings of the AIAA Guidance, Navigation, and Control Conference, **2010**.

[181] Wei, Y. H., Zhu, M., Peng, C., Wang, Y. Dynamical analysis of the deployment for a reduced spinning solar sail model. *Advances in Solar Sailing*, **2014**.

[182] Nakano, T., Mori, O., Kawaguchi, J. Stability of spinning solar sail-craft containing a huge membrane. In: Proceedings of the AIAA Guidance, Navigation, and Control Conference and Exhibit, **2005**.

[183] Funase, R., Sugita, M., Mori, O., Tsuda, Y., Kawaguchi, J. Modeling of spinning solar sail by multi particle model and its application to attitude control system. In: Proceedings of ASME 2009 International Design Engineering Technical Conferences and Computers and Information in Engineering Conference, **2009**, 983–994.

[184] Funase, R., Sugita, M., Miwa, Y., Mori, O., Kawaguchi, J. Oscillation-free attitude control of spinning solar sail with huge membrane. In: Proceedings of the 27th International Symposium on Space Technology and Science, **2009**.

[185] Okuizumi, N. Deformations and vibrations of a rotating circular membrane under distributed loads. In: Proceedings of the 48th AIAA/ASME/ASCE/AHS/ASC Structures, Structural Dynamics, and Materials Conference, **2007**.

[186] Okuizumi, N. Equilibrium of a rotating circular membrane under transverse distributed load. *Journal of System Design and Dynamics*, **2007**, 1(1): 85–96.

[187] Okuizumi, N. Vibration mode analysis of a rotating circular membrane under transverse distributed load. *Journal of System Design and Dynamics*, **2009**, 3(1): 95–106.

[188] Cerda, E., Mahadevan, L. Geometry and physics of wrinkling. *Physical Review Letters*, **2003**, 90(7): 074302.

[189] Mori, O., Shirasawa, Y., Tsuda, Y., et al. Dynamic deployment and attitude control motion of spinning solar sail "IKAROS". In: Proceedings of the 62nd International Astranautical Congress, **2011**.

[190] Sugita, M., Funase, R., Tsuda, Y., et al. Attitude control of spinning solar sail considering the deformation by solar radiation pressure. In: Proceedings of the 59th International Astranautical Congress, **2008**.

[191] Baddour, N. A modelling and vibration analysis of spinning disks. Ph.D. Dissertation, University of Toronto, Toronto, Canada, **2001**.

[192] Zhang, W., Yang, X. L. Transverse nonlinear vibrations of a circular spinning disk with a varying rotating speed. *Science China Physics, Mechanics and Astronomy*, **2010**, 53(8): 1536–1553.

[193] Tsuda, Y., Saiki, T., Funase, R., Mimasu, Y. Generalized attitude model for spinning solar sail spacecraft. *Journal of Guidance, Control, and Dynamics*, **2013**, 36(4): 967–974.

[194] Tsuda, Y., Saiki, T., Funase, R., Shirasawa, Y., Mimasu, Y. Shape parameters estimation of IKAROS solar sail using in-flight attitude determination data. In: Proceedings of the 52nd AIAA/ASME/ASCE/AHS/ASC Structures, Structural Dynamics and Materials Conference, **2011**.

[195] Tsuda, Y., Okano, Y., Mimasu, Y., Funase, R. On-orbit sail quality evaluation utilizing attitude dynamics of spinner solar sailer ikaros, *Spaceflight Mechanics*, **2012**, 143: 1609–1625.

[196] Tsuda, Y., Mimasu, Y., Funase, R., Okano, Y. Design criteria of spinning solar sail surface based on attitude dynamics. In: Proceedings of the AIAA/AAS Astrodynamics Specialist Conference, **2012**.

[197] Smith, S. W., Song, H. P., Baker, J. R., Black, J., Muheim, D. M. Flexible models for solar sail control. In: Proceedings of the 46th AIAA/ASME/ASCE/AHS/ASC Structures, Structural Dynamics & Materials Conference, **2005**.

[198] Fu, B., Farouki, R. T., Fidelis, O., Eke, O. Equilibrium configuration of a bounded inextensible membrane subject to solar radiation pressure. *Aerospace Science and Technology*, **2017**, 68: 552–560.

[199] Mansfield, E. H., Pugsley, A. G. Load Transfer via a wrinkled membrane. *Proceedings of the Royal Society of London. A. Mathematical and Physical Sciences*, **1970**, 316(1525): 269–289.

[200] Miller, R. K., Hedgepeth, J. M., Weingarten, V. I., Das, P., Kahyai, S. Finite element analysis of partly wrinkled membranes. *Computers & Structures*, **1985**, 20(1–3): 631–639.

[201] Liu, X. X., Jenkins, C. H., Schur, W. W. Large deflection analysis of pneumatic envelopes using a penalty parameter modified material model. *Finite Elements in Analysis and Design*, **2001**, 37(3): 233–251.

[202] Moriya, K., Uemura, M. An analysis of the tension field after wrinkling in flat membrane structures. In: Proceedingsof the IASS Pacific Symposium, **1971**.

[203] Fujikake, M., Kojima, O., Fukushima, S. Analysis of fabric tension structures. *Computers & Structures*, **1989**, 32(3–4): 537–547.

[204] Miyazaki, Y., Nakamura, Y. Dynamic analysis of deployable cable-membrane structures with slackening members. In: Proceedings of the 21st International Symposium on Space Technology and Science, **1998**.

[205] Roddeman, D. G., Drukker, J., Oomens, C. W. J., Janssen, J. D. The wrinkling of thin membranes: Part I—theory. *Journal of Applied Mechanics*, **1987**, 54(4): 884–887.

[206] Roddeman, D. G., Drukker, J., Oomens, C. W. J., Janssen, J. D. The wrinkling of thin membranes: Part II—numerical analysis. *Journal of Applied Mechanics*, **1987**, 54(4): 888–892.

[207] Miyazaki, Y., Uchiki, M. Deployment dynamics of inflatable tube. In: Proceedings of the 43rd AIAA/ASME/ASCE/AHS/ASC Structures, Structural Dynamics, and Materials Conference, **2002**.

[208] Sleight, D. W., Muheim, D. M. Parametric studies of square solar sails using finite element analysis. In: Proceedings of the 45th AIAA/ASME/ASCE/AHS/ASC Structures, Structural Dynamics & Materials Conference, **2004**.

[209] Sleight, D. W., Michii, Y., Lichodziejewski, D., Derbès, B., Mann, T., O. Structural analysis of an inflation-deployed solar sail with experimental validation. In: Proceedings of the 41st AIAA/ASME/SAE/ASEE Joint Propulsion Conference & Exhibit, **2005**.

[210] Miyamura, T. Wrinkling on stretched circular membrane under in-plane torsion: Bifurcation analyses and experiments. *Engineering Structures*, **2000**, 22(11): 1407–1425.

[211] Wong, Y. W. Analysis of wrinkle patterns in prestressed membrane structures. Master Dissertation, University of Cambridge, Cambridge, UK, **2000**.

[212] Papa, A., Pellegrino, S. Systematically creased thin-film membrane structures. *Journal of Spacecraft and Rockets*, **2008**, 45(1): 10–18.

[213] Pipkin, A. C. Relaxed energy densities for large deformations of membranes. *IMA Journal of Applied Mathematics*, **1994**, 52(3): 297–308.

[214] Wong, Y., W., Pellegrino, S. Computation of wrinkle amplitudes in thin membranes. In: Proceedings of the 43rd AIAA/ASME/ASCE/AHS/ASC Structures, Structural Dynamics, and Materials Conference, **2002**.

[215] Ding, H., Yang, B., Lou, M., Fang, H. A two-viable parameter membrane model for wrinkling analysis of membrane structures. In: Proceedings of the 43rd AIAA/ASME/ASCE/AHS/ASC Structures, Structural Dynamics, and Materials Conference, **2002**.

[216] Ding, H. L., Yang, B. G., Lou, M., Fang, H. F. New numerical method for two-dimensional partially wrinkled membranes. *AIAA Journal*, **2003**, 41(1): 125–132.

[217] Murphy, D. M., Murphey, T. W., Gierow, P. A. Scalable solar sail subsystem design considerations. In: Proceedings of the 43rd AIAA/ASME/ASCE/AHS/ASC Structures, Structural Dynamics, and Materials Conference, **2002**.

[218] Taleghani, B. K., Sleight, D. W., Muheim, D. M., Belvin, B., Wang, J. T. Assessment of analysis approaches for solar sail structural response. In: Proceedings of the 39th AIAA/ASME/SAE/ASEE Joint Propulsion Conference and Exhibit, **2003**.

[219] Holland, D. B. Static and dynamic characteristics of end-loaded beams with specific application in square solar sails. Ph.D. Dissertation, Duke University, Durham, UK, **2006**.

[220] Lee, K., Lee, S. W. Analysis of gossamer space structures using assumed strain formulation solid shell elements. In: Proceedings of the 43rd AIAA/ASME/ASCE/AHS/ASC Structures, Structural Dynamics, and Materials Conference, **2002**.

[221] Miyazaki, Y. Wrinkle/slack model and ?nite element dynamics of membrane. *International Journal for Numerical Methods in Engineering*, **2006**, 66(7): 1179–1209.

[222] Liu, C., Tian, Q., Yan, D., Hu, H. Y. Dynamic analysis of membrane systems undergoing overall motions, large deformations and wrinkles via thin shell elements of ANCF. *Computer Methods in Applied Mechanics and Engineering*, **2013**, 258: 81–95.

[223] Miyazaki, Y., Kodama, T. Formulation and interpretation of the equation of motion on the basis of the energy-momentum method. *Proceedings of the Institution of Mechanical Engineers, Part K: Journal of Multi-Body Dynamics*, **2004**, 218(1): 1–7.

[224] Liao, L. A study of inertia relief analysis. In: Proceedings of the 2nd AIAA/ASME/ASCE/AHS/ASC Structures, Structural Dynamics and Materials Conference, **2011**.

[225] Boni, L., Mengali, G., Quarta, A. A. Solar sail structural analysis via improved finite element modeling. *Proceedings of the Institution of Mechanical Engineers, Part G: Journal of Aerospace Engineering*, **2017**, 231(2): 306–318.

[226] Potes, F. C. General conceptual design problems of a parabolic solar sail structure. Universidade da Beira Interior, **2012**.

[227] Choi, M., Damaren, C. J. Structural dynamics and attitude control of a solar sail using tip vanes. *Journal of Spacecraft and Rockets*, **2015**, 52(6): 1665–1679.

[228] Yamazaki, M., Miyazaki, Y. Low-order model of spin type solar sail dynamics by empirical model reduction. In: Proceedings of the 52nd AIAA/ASME/ASCE/AHS/ASC Structures, Structural Dynamics and Materials Conference, **2011**.

[229] Yamazaki, M., Miyazaki, Y. Error estimation of low-order model for gossamer multi-body structure. In: Proceedings of the AIAA Modeling and Simulation Technologies Conference, **2011**.

[230] Chen, S. H., Pan, H. H. Guyan reduction. *International Journal for Numerical Methods in Biomedical Engineering*, **1988**, 4(4): 549–556.

[231] Li, Q., Ma, X. R., Wang, T. S. Reduced model for flexible solar sail dynamics. *Journal of Spacecraft and Rockets*, **2011**, 48(3): 446–453.

[232] Miyazaki, Y., Iwai, Y. Dynamics model of solar sail membrane. In: Proceedings of the 14th Workshop on Astrodynamics and Flight Mechanics, **2004**.

[233] Okuizumi, N. Numerical simulations of centrifugal deployments of membranes by spring-mass system models. In: Proceedings of the 51st AIAA/ASME/ASCE/AHS/ASC Structures, Structural Dynamics, and Materials Conference, **2010**.

[234] Okuizumi, N., Yamamoto, T. Centrifugal deployment of membrane with spiral folding: Experiment and simulation. *Journal of Space Engineering*, **2009**, 2(1): 41–50.

[235] Shirasawa, Y., Mori, O., Miyazaki, Y., Sakamoto, H., Hasome, M., Okuizumi, N., Sawada, H., Furuya, H., Matsunaga, S., Natori, N. et al. Analysis of membrane dynamics using multi-particle model for solar sail demonstrator "IKAROS". In: Proceedings of the 52nd AIAA/ASME/ASCE/AHS/ASC Structures, Structural Dynamics and Materials Conference, **2011**.

[236] Shirasawa, Y., Mori, O., Sawada, H., Chishiki, Y., Kitamura, K., Kawaguchi, J. A study on membrane dynamics and deformation of solar power sail demonstrator "IKAROS". In: Proceedings of the 53rd AIAA/ASME/ASCE/AHS/ASC Structures, Structural Dynamics and Materials Conference, **2012**.

[237] Johnson, M., McCann, J., Santer, M., Baoyin, H., Gong, S. P. On orbit validation of solar sailing control laws with thin-film spacecraft. In: Proceedings of the 4th International Symposium on Solar Sailing, **2017**.

[238] Janson, S., Brane craft. NIAC 2016 phase 1 Janson Brane Craft final report. Available at: https://www.nasa.gov/sites/default/files/atoms/files/niac_2016_phasei_janson_braneconcept_tagged.pdf.

Shengping Gong received his Ph.D. degree in mechanical engineering from Tsinghua University, China, in 2008. He is an associate professor at School of Aerospace Engineering, Tsinghua University. His research interests cover the solar sailing, dynamics of many-body system, and manned space flight. E-mail: gongsp@tsinghua.edu.cn.

Malcolm Macdonald is a professor of mechanical and aerospace engineering at University of Strathclyde, Glasgow. He is the director of the Scottish Centre of Excellence in Satellite Applications, and a non-executive board member of the UK Space Agency. He was awarded the 2016 Royal Society of Edinburgh Sir Thomas Makdougall Brisbane Medal. He was the only non-US member of a National Academies of Sciences, Engineering, and Medicine's committee on "Achieving Science Goals with CubeSats", and one of only two European associate editors of the *Journal of Guidance, Control, and Dynamics*. His research interests are in the use of advanced concepts, such as solar sailing, and multi-spacecraft platforms, to enable new space services through the application of concepts from networked systems and swarm engineering, combined with astrodynamics and space system design. E-mail: malcolm.macdonald.102@strath.ac.uk.